SANDIA REPORT
SAND2021-14813
Printed November 2021

Sandia National Laboratories

Hydrogen Plus Other Alternative Fuels Risk Assessment Models (HyRAM+) Version 4.0 Technical Reference Manual

Updated by: Ethan S. Hecht and Brian D. Ehrhart

Previous Contributors (chronological): Katrina M. Groth, Ethan S. Hecht, John T. Reynolds, Myra L. Blaylock, Erin E. Carrier, and Brian D. Ehrhart

Prepared by
Sandia National Laboratories
Albuquerque, New Mexico 87185
Livermore, California 94550

Issued by Sandia National Laboratories, operated for the United States Department of Energy by National Technology & Engineering Solutions of Sandia, LLC.

Available to DOE and DOE contractors from

U.S. Department of Energy
Office of Scientific and Technical Information
P.O. Box 62
Oak Ridge, TN 37831

Telephone: (865) 576-8401
Facsimile: (865) 576-5728
E-Mail: reports@osti.gov
Online ordering: http://www.osti.gov/scitech

Available to the public from

U.S. Department of Commerce
National Technical Information Service
5301 Shawnee Road
Alexandria, VA 22312

Telephone: (800) 553-6847
Facsimile: (703) 605-6900
E-Mail: orders@ntis.gov
Online order: https://classic.ntis.gov/help/order-methods

ABSTRACT

The HyRAM+ software toolkit provides a basis for conducting quantitative risk assessment and consequence modeling for hydrogen, methane, and propane infrastructure and transportation systems. HyRAM+ is designed to facilitate the use of state-of-the-art science and engineering models to conduct robust, repeatable assessments of safety, hazards, and risk. HyRAM+ includes generic probabilities for equipment failures, probabilistic models for the impact of heat flux on humans and structures, and experimentally validated first-order models of release and flame physics. HyRAM+ integrates deterministic and probabilistic models for quantifying accident scenarios, predicting physical effects, and characterizing hazards (thermal effects from jet fires, overpressure effects from delayed ignition), and assessing impact on people and structures. HyRAM+ is developed at Sandia National Laboratories to support the development and revision of national and international codes and standards. HyRAM+ is a research software in active development and thus the models and data may change. This report will be updated at appropriate developmental intervals.

This document provides a description of the methodology and models contained in HyRAM+ version 4.0. The most significant change for HyRAM+ version 4.0 from HyRAM version 3.1 is the incorporation of other alternative fuels, namely methane (as a proxy for natural gas) and propane into the toolkit. This change necessitated significant changes to the installable graphical user interface as well as changes to the back-end Python models. A second major change is the inclusion of physics models for the overpressure associated with the delayed ignition of an unconfined jet/plume of flammable gas.

ACKNOWLEDGMENT

This report describes HyRAM+, a revised version of the HyRAM code, which itself was built upon the previous work of many others. The authors therefore especially wish to thank Katrina Groth (now at the University of Maryland) for her leadership and contributions to the HyRAM code and project, as well as John Reynolds, and Erin Carrier for their contributions. The authors also wish to thank Benjamin B. Schroeder of Sandia, Cianan Sims of Sims Industries, and Jeremey Rifkin for their contributions to the HyRAM+ code. This work was supported by the U.S. Department of Energy (DOE) Office of Energy Efficiency (EERE) Hydrogen and Fuel Cell Technologies Office (HFTO), the DOE EERE's Vehicles Technologies Office (VTO), and the U.S. Department of Transportation's Pipeline and Hazardous Materials Safety Administration (PHMSA). The authors gratefully acknowledge Myra Blaylock, Chris LaFleur, Dusty Brooks, and Alice Muna at Sandia for helpful discussions and useful insights. The authors also wish to specifically thank the members of NFPA 2, the Hydrogen Safety Panel, and HySafe for engaging technical discussions and thoughtful feedback. Finally, the authors gratefully acknowledge the many productive discussions with users, other researchers, and the various stakeholders who have provided insight and feedback for this work.

CONTENTS

LIST OF FIGURES

LIST OF TABLES

ACRONYMS AND DEFINITIONS

AIR average individual risk

C&S codes and standards

CFD computational fluid dynamics

CNG compressed natural gas

DOE U.S. Department of Energy

EERE Office of Energy Efficiency and Renewable Energy

ESD event sequence diagram

FAR fatal accident rate

H_2 hydrogen

HFTO Hydrogen and Fuel Cell Technologies Office

HSE U.K. Health and Safety Executive

HyRAM Hydrogen Risk Assessment Models

HyRAM+ Hydrogen Plus Other Alternative Fuels Risk Assessment Models

ISO International Organization for Standardization

LNG liquid natural gas

MW molecular weight

NG natural gas

NFPA National Fire Protection Association

PLL potential loss of life

QRA quantitative risk assessment

SI International System of Units

TNO Netherlands Organisation for Applied Scientific Research

TNT trinitrotoluene

1. INTRODUCTION

1.1. About HyRAM+ and This Report

HyRAM+ (Hydrogen Plus Other Alternative Fuels Risk Assessment Models) is a software toolkit that integrates data and methods relevant to assessing the safety in the use, delivery, and storage infrastructure of hydrogen and other alternative fuels (i.e., natural gas and propane). HyRAM+ provides a platform which integrates state-of-the-art, validated science and engineering models and data relevant to safety into a comprehensive, industry-focused platform. The HyRAM+ risk assessment calculation incorporates generic probabilities for equipment failures for different components for both compressed gaseous and liquefied fuels, and probabilistic models for the effect of heat flux and overpressure on humans and structures. HyRAM+ also incorporates experimentally validated models of various aspects of release and flame physics. The HyRAM+ toolkit can be used to support multiple types of analysis, including code and standards development, safety basis development, and facility safety planning. HyRAM+ is an extension of HyRAM, which was developed by Sandia National Laboratories for the U.S. Department of Energy (DOE) Office of Energy Efficiency and Renewable Energy (EERE) Hydrogen and Fuel Cell Technologies Office (HFTO) [1]. The inclusion of other alternative fuels into HyRAM+ has been supported by the DOE EERE's Vehicle Technologies Office (VTO) as well as the U.S. Department of Transportation's Pipeline and Hazardous Materials Safety Administration (PHMSA).

This report provides technical documentation of the algorithms, models, and data incorporated in HyRAM+ version 4.0. HyRAM+ is free and open source software: you can redistribute it and/or modify it under the terms of the GNU General Public License version 3, as published by the Free Software Foundation. This program is distributed in the hope that it will be useful, but WITHOUT ANY WARRANTY; without even the implied warranty of MERCHANTABILITY or FITNESS FOR A PARTICULAR PURPOSE. See the GNU General Public License for more details (`https://www.gnu.org/licenses/gpl-3.0.html`).

1.2. Design Goals and Limitations

HyRAM+ is designed to calculate multiple risk and harm/damage metrics from user-defined system configurations to provide insights for decision makers in the safety, codes, and standards community. HyRAM+ contains generic industry-wide default inputs and fast-running, reduced-order models designed to facilitate comparison of different system designs and requirements. Reduced-order models use simplifying assumptions to approximate behavior much more quickly than more complex high-fidelity models. As such, the focus of HyRAM+ is on enabling systematic, defensible risk and consequence assessments for use in risk comparisons and sensitivity analyses, rather than on establishing the "true" frequency or risk of a hypothetical accident. HyRAM+ is designed to produce realistic best estimates for use in decision-making.

Note: Risk and safety assessment results should be used as part of a decision process, not as the sole basis for a decision. Safety and design decisions involve consideration of many factors and

judgments; these factors include the safety assessments, the assumptions and limitations of safety assessments, the benefits of a technology, and public preferences. As such, HyRAM+ does not allow the user to specify an acceptability or tolerability criteria for risk or harm. Further guidance on QRA and tolerability criteria can be found in the references [2–9].

HyRAM+ is designed to enable defensible, repeatable calculations using consistent, documented algorithms. The algorithms, models, and data in HyRAM+ have been assembled from published, publicly available sources. The physics models contained in HyRAM+ have been validated against available experimental data [10–13]. Where model validation is not possible (e.g., for harm models), HyRAM+ is designed to allow users to choose among different models. HyRAM+ includes generic data for component leak frequencies, which are in most cases specific to the fuel (leak frequency analyses have been completed for compressed, liquid hydrogen and liquid natural gas, while generic data was used to determine frequencies for CNG and propane). HyRAM+ also includes documented, expert-assigned probabilities for ignition. HyRAM+ is designed to allow users to replace the default parameters (e.g. leak frequency distribution parameters for every component) and assumptions with system-specific information when such information is available to the user.

1.3. Summary of HyRAM+ Outputs

The QRA mode in HyRAM+ can be used to calculate three well-known risk metrics which are commonly used to evaluate fatality risk in multiple industries, as well as other risk-related metrics:

- FAR (Fatal Accident Rate) – the expected number of fatalities in 100 million exposed hours;
- AIR (Average Individual Risk) – the expected number of fatalities per exposed individual;
- PLL (Potential Loss of Life) – the expected number of fatalities per system-year;
- Expected number of releases per system-year (unignited and ignited cases);
- Expected number of jet fires per system-year (immediate ignition cases);
- Expected number of deflagrations/explosions per system-year (delayed ignition cases).

The physics mode of HyRAM+ can be used to calculate multiple physical effects associated with hydrogen, methane, and propane, including:

- Concentration for an unignited plume;
- Jet flame temperature and trajectory;
- Jet flame radiative heat flux (kW/m^2) at user-defined positions;
- Contours of distance to user-defined heat flux levels from jet flames;
- Time histories of concentration, flammable mass, and overpressure due to accumulation and delayed ignition in an enclosure;
- The overpressure as a function of distance that would result from the delayed ignition of a jet/plume.

1.4. Summary of Changes Made

HyRAM+ is an open source software, meaning that changes to the code can be observed directly[1]. However, a summary of major changes made to the models will be included here for ease of reference.

The most significant change for HyRAM+ version 4.0 from HyRAM version 3.1 is the incorporation of other alternative fuels, namely methane and propane into the toolkit. This change necessitated significant changes to the installable graphical user interface as well as changes to the back-end Python models. A second major change is the inclusion of models for an additional physical phenomenon, namely the overpressure associated with the delayed ignition of an unconfined jet/plume of flammable gas.

Other changes include:

- Added additional components (specifically for liquid fuels) in QRA mode
- Updated/added fuel-specific leak frequencies for hydrogen (liquid and gas), methane (liquid and gas), and propane
- Added fuel-specific critical pressure check for saturated liquid or saturated vapor calculations
- Added mass flow rate graph for indoor accumulation model
- Added Python tests for QRA mode and unconfined overpressure models
- Added/clarified scenario details in QRA results
- Added positional heat flux table in QRA results
- Flame temperature/trajectory model output tab now displays mass flow rate and total emitted power
- The overpressure physics model was renamed to accumulation to differentiate from unconfined overpressure model
- The occupant location calculation was simplified in QRA mode
- The TNT equivalent model in the Engineering Toolkit now looks up heat of combustion for specific fuels
- Plot labels specific to hydrogen were changed to “fuel”
- The secondary orifice area was removed from the accumulation physics model
- Improved warning and error notifications
- Data directory now cleared on program launch to avoid excessive disk usage

[1] More detailed changes are given in the source code changelog: `https://github.com/sandialabs/hyram/blob/master/CHANGELOG.md`

This page intentionally left blank.

2. QUANTITATIVE RISK ASSESSMENT METHODOLOGY

HyRAM+ includes a QRA mode, which provides calculations and models relevant to estimating the risk of infrastructure for hydrogen and other alternative fuels. The consequences and fatality risk of jet flames and overpressures are estimated for different release sizes, each of which can be calculated to occur with different frequencies. These calculations use a subset of the models used in the physics mode to estimate the release behavior (see Section 3).

2.1. Quantitative Risk Assessment Methodology Overview

In a QRA, multiple integrated models are used to provide a framework for reasoning about decision options, based on the background information encoded in those models.

Risk is characterized by a set of hazard exposure scenarios (i), the consequences (c_i) associated with each scenario, and the probability of occurrence (p_i) of these consequences. One commonly used expression for calculating risk is:

$$\text{Risk} = \sum_i (p_i \times c_i) \tag{1}$$

In a QRA, the consequences are expressed in terms of an observable quantity, such as number of fatalities or repair cost in a specific period of time. In HyRAM+, the number of fatalities is used as the safety metric of interest.

The major elements of the QRA methodology in HyRAM+ are shown in Figure 2-1.

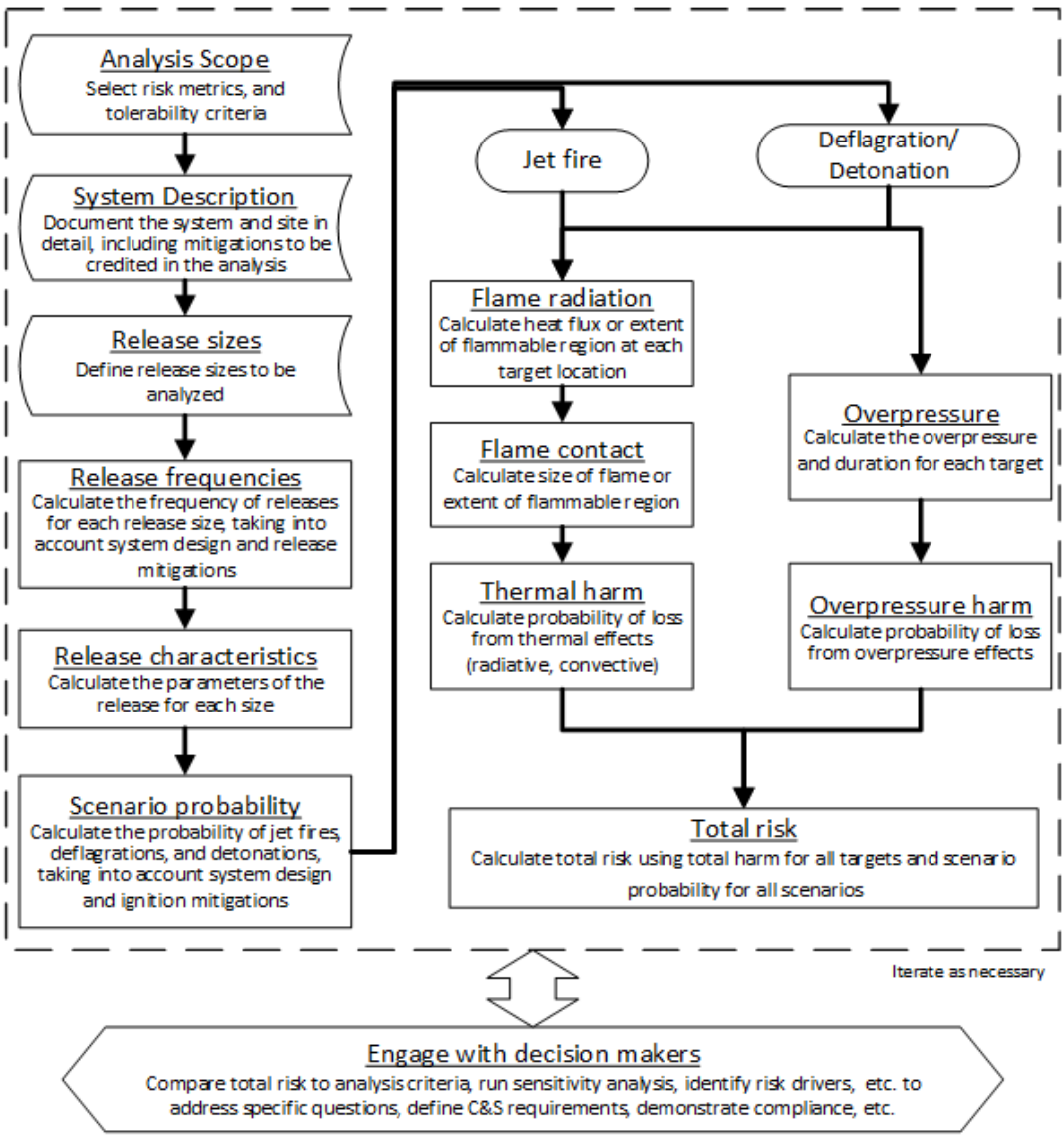

Figure 2-1 Summary of QRA methodology implemented in HyRAM+ toolkit

2.2. Risk Metrics Calculations

There are multiple metrics used to express the fatality risk for a system under consideration. One such metric is the Potential Loss of Life (PLL). The PLL expresses the expected number of fatalities per system-year. The PLL is expressed as follows:

$$\mathrm{PLL} = \sum_{n} (f_n \times c_n) \tag{2}$$

where n is one of the possible safety-significant scenarios (described in Section 2.3), f_n is the frequency of that accident scenario n (described in Sections 2.3 and 2.4), and c_n is the expected

number of fatalities for accident scenario n (described in Section 2.6).

Another metric related to the PLL is the Fatal Accident Rate (FAR). The FAR is the expected number of fatalities in a group, per 100 million exposed hours. The FAR for a particular facility can be calculated using the PLL, as well as the population of the facility. The FAR is calculated using Equation 3.

$$\text{FAR} = \frac{\text{PLL} \times 10^8}{\text{Exposed hours}} = \frac{\text{PLL} \times 10^8}{N_{pop} \times 8760} \tag{3}$$

where N_{pop} is the average number of personnel in the facility, and dividing by 8760 converts from years to hours (24 hours per day and 365 days per year).

The third metric used in HyRAM+ is the Average Individual Risk (AIR). The AIR expresses the average number of fatalities per exposed individual. It is based on the number of hours the average occupant spends at the facility.

$$\text{AIR} = H \times \text{FAR} \times 10^{-8} \tag{4}$$

where H is the annual number of hours the individual spends in the facility (e.g., 2000 hours for full-time worker).

2.3. Scenario Models

A release of a flammable fuel could lead to several different physical consequences and associated hazards. For continuous releases of a fuel, the physical consequences are unignited releases, jet fires (thermal effects), flash fires (deflagration of accumulated gas, dominated by thermal effects), and explosions (deflagration or detonation of accumulated gas dominated by overpressure effects). Currently, HyRAM+ calculates harm from thermal effects of jet fires (for immediate ignition) and overpressure (for delayed ignition)[2]. A release of a liquid fuel (e.g. liquid hydrogen or liquid natural gas) may also form a pool on the ground, but this is currently not considered in HyRAM+. These scenarios are modeled in the event sequence diagram (ESD) for release of a flammable fuel (see Figure 2-2).

[2]Future versions of HyRAM+ may take account for the differences between thermal effects and overpressure effects for delayed ignition, but this is not currently included.

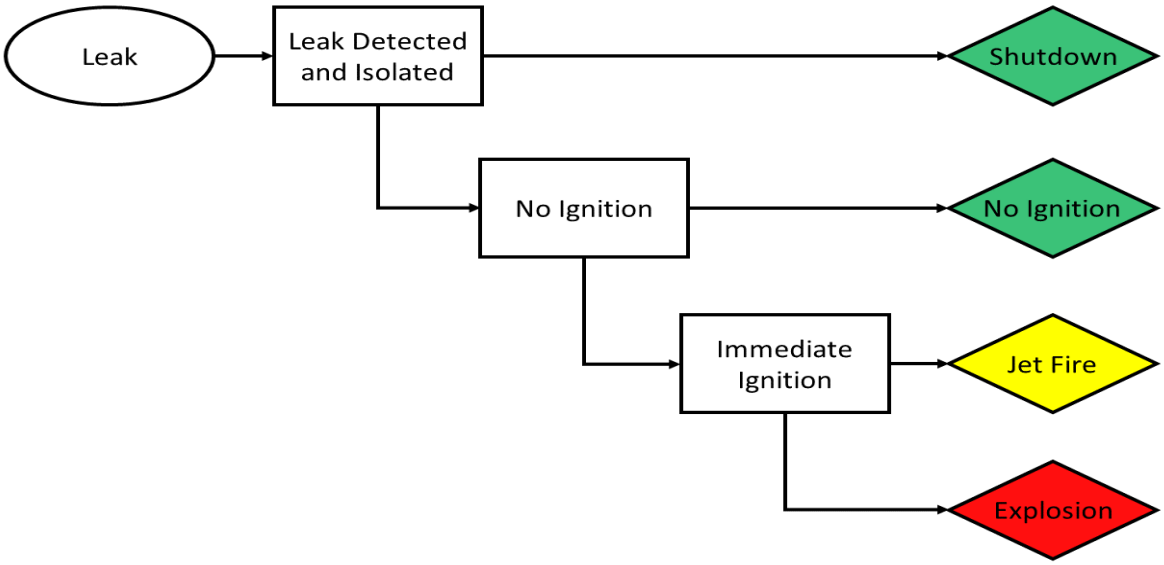

Figure 2-2 Event sequence diagram used by HyRAM+ for flammable gas releases

The ESD is encoded in HyRAM+ using the following equations[3]:

$$f_{\text{Isolated}} = f_{\text{Release}} \times P(\text{Isolated}) \tag{5}$$

$$f_{\text{Unignited}} = f_{\text{Release}} \times P(\overline{\text{Isolated}}) \times (1 - P(\text{Immed. Ignite}) - P(\text{Delayed Ignite})) \tag{6}$$

$$f_{\text{Jetfire}} = f_{\text{Release}} \times P(\overline{\text{Isolated}}) \times P(\text{Immed. Ignite}) \tag{7}$$

$$f_{\text{Explosion}} = f_{\text{Release}} \times P(\overline{\text{Isolated}}) \times P(\text{Delayed Ignite}) \tag{8}$$

where f_{Release} is the annual frequency of a release (see Section 2.4), $P(\text{Isolated})$ is the probability of release (leak) detection and isolation before ignition (see Section 2.3.1), $P(\text{Immed. Ignite})$ is the probability of immediate ignition (see Section 2.3.2), and $P(\text{Delayed Ignite})$ is the probability of delayed ignition (see Section 2.3.2). The equations are written in this way so as to utilize ignition probabilities that are given all relative to a leak, not as conditional probabilities relative to each other.

2.3.1. Default Detection and Isolation Probability

The default value for successful detection and isolation of a release, $P(\text{Isolate})$, is 0.9. This value incorporates many considerations on detection and isolation including: ventilation, sensor placement, leak location, and the ability of the sensor and isolation valve to operate successfully on demand. This default value was chosen in a previous analysis [14] specific to hydrogen as a general rough estimate while acknowledging significant uncertainty.

[3]Notation: $P(\text{event})$ is the probability of occurrence of the event; $P(\overline{\text{event}})$ means the probability of non-occurrence of an event, which is equal to $P(\overline{\text{event}}) = 1 - P(\text{event})$

Note: This value can vary significantly based on a particular system setup, and so the user/analyst needs to carefully consider the particulars of the system being assessed and decide if this default value is appropriate.

2.3.2. Default Ignition Probabilities

The default ignition probabilities are a function of release rate and are given in Table 2-1; these values are taken directly from [15], with efforts underway to generate more scientifically defensible probabilities. It should be noted that both the immediate and delayed ignition probabilities are independent and both relative to a release; the delayed ignition probability is not conditional upon the immediate ignition having not occurred. The total probability of ignition is the immediate and delayed ignition probabilities added together. Note that in HyRAM+ 4.0, the default ignition probabilities for methane and propane (i.e., the values in Table 2-1(b)) do not auto-populate upon fuel change (i.e., the values in Table 2-1(a) remain in the software). The user will need to manually update the ignition probability table for these fuels.

Table 2-1 Ignition Probabilities

(a) Hydrogen

Release Rate (kg/s)	Ignition Probability	
	Immediate	Delayed
<0.125	0.008	0.004
0.125 – 6.25	0.053	0.027
>6.25	0.230	0.120

(b) Methane and Propane

Release Rate (kg/s)	Ignition Probability	
	Immediate	Delayed
<1	0.007	0.003
1 – 50	0.047	0.023
>50	0.200	0.100

2.4. Frequency of a Release

HyRAM+ calculates the annual frequency of a release for release sizes of 0.01%, 0.1%, 1%, 10%, or 100%. These release sizes are relative to the pipe flow area (A) as shown in Equation 9, where d is the inner diameter of the pipe[4].

$$A = \frac{\pi}{4} d^2 \tag{9}$$

The annual frequency of a release for each of the four smallest releases sizes ($k = 0.01\%$, 0.1%, 1%, and 10%) is only due to random leaks (see Section 2.4.1), i.e.

$$f_{\text{Release,k}} = f_{\text{Random Releases},k} \tag{10}$$

The annual frequency of the largest release size (100%) is due to both random leaks (see Section 2.4.1) and other releases (see Section 2.4.3), i.e.

$$f_{\text{Release, k=100\%}} = f_{\text{Random Releases},k=100\%} + f_{\text{Other Releases}} \tag{11}$$

[4]In many fluid flow calculations, a discharge coefficient is used to scale the mass flow through an orifice, effectively reducing the flow area. The discharge coefficient used in QRA mode is 1.0 and cannot currently be changed.

2.4.1. Frequency of Random Leaks

The annual frequency of random leaks is obtained for each release size using a fault tree. As an example, the fault tree for random leaks for leak size 0.01% is shown in Figure 2-3. The fault trees for random leaks for all other leak sizes are analagous per leak size.

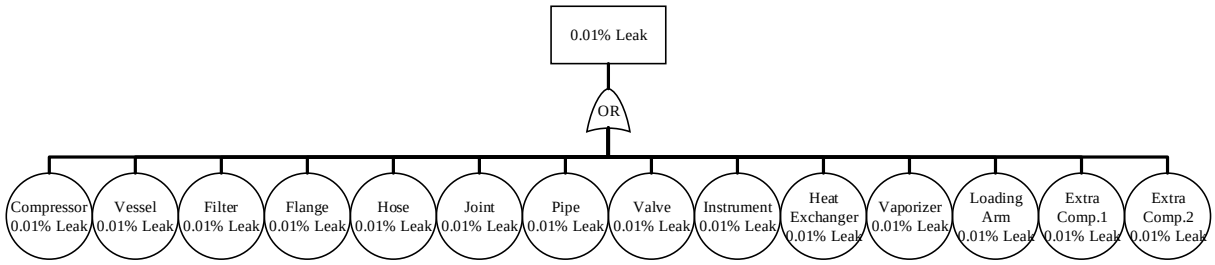

Figure 2-3 Fault tree for random leaks of size 0.01% from components

The fault trees are encoded in HyRAM+ to combine component leak frequencies into an overall leak frequency for each size. The annual frequency of random leaks ($f_{\text{Random Releases},k}$) is calculated for each release of size k by combining the individual component leak frequencies for all the components in the system of interest:

$$f_{\text{Random Releases},k} = \sum_i N_{\text{Component}_i} \times f_{\text{Leak}_{i,k}} \tag{12}$$

where $N_{\text{Component}_i}$ is the number of components of each type and $f_{\text{Leak}_{i,k}}$ is the geometric mean leak frequency of size k for component i (see Section 2.4.2). The component types are Vessels (Cylinders/Tanks), Compressors, Flanges, Hoses, Joints, Pipes[5], Valves, Filters, Instruments, Heat Exchangers, Loading Arms, Vaporizers, Extra Component #1, and Extra Component #2. Some of these components are only used for gaseous fuels (e.g. Compressors), while some are only used for liquid fuels (e.g. Pumps), although all are available for either gaseous or liquid fuels.

2.4.2. Default Component Leak Frequencies

In HyRAM+, the annual frequency of a random leak (f_{Leak}) is assumed to be distributed as a lognormal distribution with parameters μ and σ:

$$f_{\text{Leak}} \sim \text{Lognormal}(\mu, \sigma^2) \tag{13}$$

The geometric mean (which is equal to the median) is given by:

[5]The "Pipes" component type is per-meter of pipe; so if a system has 15 m worth of piping, then the "number" of components for that type is 15.

$$\text{median} = e^{\mu} \tag{14}$$

The geometric mean (median) values are used in the frequency calculations in HyRAM+ as a metric of central-tendency for the distribution.

The default values for compressed hydrogen are based on generic system leak frequencies and data from compressed hydrogen systems developed by LaChance et al. [16] and updated by both Groth et al. [14] and Glover et al. [17]. For liquid hydrogen, leak frequencies were determined using gaseous hydrogen and LNG data as outlined by Brooks et al. [18]. For compressed natural gas and propane, the generic system leak frequencies described by LaChance et al. [16] (without the update using hydrogen data) are used. For liquid methane, the analysis described by Mulcahy et al. [19] was used. In each case, a distribution of approximately 2.5 million leak frequencies for each component were generated from a hierarchical Bayesian model assuming a lognormal distribution. From the model output, the median leak rate was found, and μ was calculated as $\ln(\text{median})$. The standard deviation, σ, was calculated from the simulated data as

$$\sigma = \frac{\sqrt{\sum_{i=1}^{N} (\ln x_i - \mu)^2}}{N} \tag{15}$$

where x_i is each leak frequency in the simulated distribution. Note that these fits to the Bayesian model data have resulted in slightly updated median leak frequencies for gaseous hydrogen than for previous versions of the HyRAM software. The default leak frequency distributions for each component are shown in Fig. 2-4 and the parameters and median values for the distributions are listed in Table 2-2.

In HyRAM+ 4.0, only the geometric mean (median) leak frequency is used in release calculations based on lognormal distributions. Future versions of HyRAM+ may be designed to use additional information from the lognormal distribution in uncertainty propagation.

There are two extra components: Extra Component #1 and Extra Component #2 which might not fall into the other component type categories. The intention is that users can specify a custom leak frequency distribution for these components while still keeping the leak frequency distributions for the other components. These are meant to be set by the user. For each component for which there is no data for a specific fuel, the mean and median leak frequencies are set to infinity, with μ and σ set to 999 to achieve this effect. If a user has data for these components for a specific fuel, they can be updated. By making the default median frequency infinity, the risk metric will end up at infinity if one of these components is included in the system.

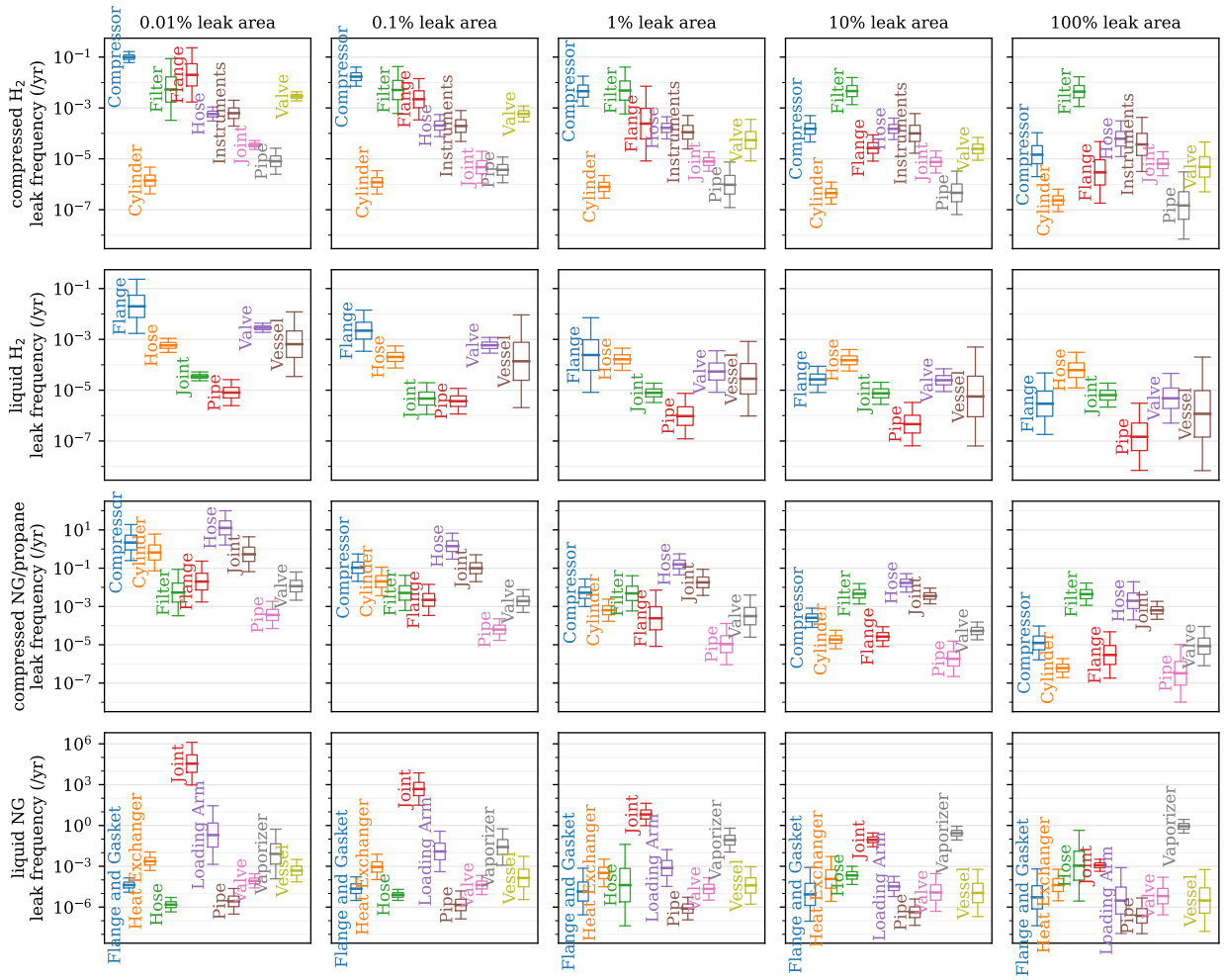

Figure 2-4 Box and whisker plots of leak frequencies for the different components (colors) for each fuel (rows) at each leak size (columns). Each component is labeled with its type, the thick central line is the median leak frequency, the boxes show the 25th and 75th percentiles of the distribution and the whiskers show the 5th and 95th percentiles.

Table 2-2 Default parameters for frequency of random leaks for individual components

Component	Leak Size	Compressed H_2			Liquid H_2			Compressed NG / Propane			Liquid NG		
		μ	σ	median	μ	σ	median	μ	σ	median	μ	σ	median
Compressor	0.01%	-2.31	0.30	9.97×10^{-2}	NaN	NaN	NaN	0.78	1.32	2.18×10^{0}	NaN	NaN	NaN
	0.1%	-4.08	0.52	1.70×10^{-2}	NaN	NaN	NaN	-2.24	1.00	1.07×10^{-1}	NaN	NaN	NaN
	1%	-5.39	0.82	4.57×10^{-3}	NaN	NaN	NaN	-5.26	1.01	5.22×10^{-3}	NaN	NaN	NaN
	10%	-8.79	0.73	1.52×10^{-4}	NaN	NaN	NaN	-8.27	0.70	2.55×10^{-4}	NaN	NaN	NaN
	100%	-11.14	1.21	1.46×10^{-5}	NaN	NaN	NaN	-11.29	1.23	1.25×10^{-5}	NaN	NaN	NaN
Cylinder	0.01%	-13.48	0.73	1.40×10^{-6}	NaN	NaN	NaN	-0.41	1.34	6.61×10^{-1}	NaN	NaN	NaN
	0.1%	-13.64	0.64	1.19×10^{-6}	NaN	NaN	NaN	-3.90	1.04	2.03×10^{-2}	NaN	NaN	NaN
	1%	-14.05	0.62	7.90×10^{-7}	NaN	NaN	NaN	-7.36	0.81	6.35×10^{-4}	NaN	NaN	NaN
	10%	-14.61	0.60	4.50×10^{-7}	NaN	NaN	NaN	-10.88	0.68	1.88×10^{-5}	NaN	NaN	NaN
	100%	-15.27	0.62	2.33×10^{-7}	NaN	NaN	NaN	-14.32	0.69	6.06×10^{-7}	NaN	NaN	NaN
Filter	0.01%	-5.23	1.70	5.33×10^{-3}	NaN	NaN	NaN	-5.23	1.70	5.33×10^{-3}	NaN	NaN	NaN
	0.1%	-5.28	1.29	5.08×10^{-3}	NaN	NaN	NaN	-5.28	1.29	5.08×10^{-3}	NaN	NaN	NaN
	1%	-5.33	1.29	4.84×10^{-3}	NaN	NaN	NaN	-5.33	1.29	4.84×10^{-3}	NaN	NaN	NaN
	10%	-5.38	0.74	4.61×10^{-3}	NaN	NaN	NaN	-5.38	0.74	4.61×10^{-3}	NaN	NaN	NaN
	100%	-5.43	0.82	4.39×10^{-3}	NaN	NaN	NaN	-5.43	0.82	4.39×10^{-3}	NaN	NaN	NaN
Flange	0.01%	-3.91	1.49	2.00×10^{-2}	-3.91	1.49	2.00×10^{-2}	-3.91	1.49	2.00×10^{-2}	NaN	NaN	NaN
	0.1%	-6.12	1.13	2.20×10^{-3}	-6.12	1.13	2.20×10^{-3}	-6.12	1.13	2.20×10^{-3}	NaN	NaN	NaN
	1%	-8.33	2.05	2.42×10^{-4}	-8.33	2.05	2.42×10^{-4}	-8.33	2.05	2.42×10^{-4}	NaN	NaN	NaN
	10%	-10.53	0.72	2.67×10^{-5}	-10.53	0.72	2.67×10^{-5}	-10.53	0.72	2.67×10^{-5}	NaN	NaN	NaN
	100%	-12.74	1.69	2.94×10^{-6}	-12.74	1.69	2.94×10^{-6}	-12.74	1.69	2.94×10^{-6}	NaN	NaN	NaN
Flange and Gasket	0.01%	NaN	NaN	NaN	NaN	NaN	NaN	NaN	NaN	NaN	-10.08	0.73	4.18×10^{-5}
	0.1%	NaN	NaN	NaN	NaN	NaN	NaN	NaN	NaN	NaN	-10.70	1.21	2.26×10^{-5}
	1%	NaN	NaN	NaN	NaN	NaN	NaN	NaN	NaN	NaN	-11.18	2.40	1.40×10^{-5}
	10%	NaN	NaN	NaN	NaN	NaN	NaN	NaN	NaN	NaN	-11.66	2.76	8.64×10^{-6}
	100%	NaN	NaN	NaN	NaN	NaN	NaN	NaN	NaN	NaN	-12.16	2.91	5.24×10^{-6}
Heat Exchanger	0.01%	NaN	NaN	NaN	NaN	NaN	NaN	NaN	NaN	NaN	-6.06	0.96	2.34×10^{-3}
	0.1%	NaN	NaN	NaN	NaN	NaN	NaN	NaN	NaN	NaN	-7.02	1.30	8.95×10^{-4}
	1%	NaN	NaN	NaN	NaN	NaN	NaN	NaN	NaN	NaN	-8.03	1.42	3.24×10^{-4}
	10%	NaN	NaN	NaN	NaN	NaN	NaN	NaN	NaN	NaN	-9.05	2.31	1.17×10^{-4}
	100%	NaN	NaN	NaN	NaN	NaN	NaN	NaN	NaN	NaN	-10.08	1.62	4.18×10^{-5}
Hose	0.01%	-7.45	0.39	5.79×10^{-4}	-7.45	0.39	5.79×10^{-4}	2.54	1.25	1.27×10^{1}	-13.40	0.74	1.52×10^{-6}
	0.1%	-8.50	0.60	2.03×10^{-4}	-8.50	0.60	2.03×10^{-4}	0.35	0.94	1.41×10^{0}	-11.75	0.56	7.89×10^{-6}
	1%	-8.71	0.61	1.65×10^{-4}	-8.71	0.61	1.65×10^{-4}	-1.84	0.77	1.58×10^{-1}	-10.09	4.19	4.13×10^{-5}
	10%	-8.80	0.59	1.51×10^{-4}	-8.80	0.59	1.51×10^{-4}	-4.07	0.67	1.70×10^{-2}	-8.45	0.93	2.13×10^{-4}
	100%	-9.69	0.98	6.17×10^{-5}	-9.69	0.98	6.17×10^{-5}	-6.23	1.39	1.98×10^{-3}	-6.81	3.64	1.11×10^{-3}
Instruments	0.01%	-7.38	0.71	6.24×10^{-4}	NaN	NaN	NaN	NaN	NaN	NaN	NaN	NaN	NaN
	0.1%	-8.54	0.85	1.95×10^{-4}	NaN	NaN	NaN	NaN	NaN	NaN	NaN	NaN	NaN
	1%	-9.10	0.92	1.12×10^{-4}	NaN	NaN	NaN	NaN	NaN	NaN	NaN	NaN	NaN
	10%	-9.21	1.09	1.00×10^{-4}	NaN	NaN	NaN	NaN	NaN	NaN	NaN	NaN	NaN
	100%	-10.21	1.49	3.68×10^{-5}	NaN	NaN	NaN	NaN	NaN	NaN	NaN	NaN	NaN
Joint	0.01%	-10.26	0.24	3.50×10^{-5}	-10.26	0.24	3.50×10^{-5}	-0.63	1.27	5.35×10^{-1}	10.47	2.20	3.51×10^{4}
	0.1%	-12.27	0.87	4.69×10^{-6}	-12.27	0.87	4.69×10^{-6}	-2.31	0.98	9.96×10^{-2}	6.17	1.66	4.77×10^{2}
	1%	-11.75	0.53	7.86×10^{-6}	-11.75	0.53	7.86×10^{-6}	-4.01	0.95	1.81×10^{-2}	1.87	1.15	6.46×10^{0}
	10%	-11.80	0.61	7.53×10^{-6}	-11.80	0.61	7.53×10^{-6}	-5.65	0.57	3.52×10^{-3}	-2.43	0.71	8.76×10^{-2}
	100%	-11.96	0.66	6.40×10^{-6}	-11.96	0.66	6.40×10^{-6}	-7.37	0.66	6.27×10^{-4}	-6.74	0.62	1.19×10^{-3}
Loading Arm	0.01%	NaN	NaN	NaN	NaN	NaN	NaN	NaN	NaN	NaN	-1.62	3.01	1.99×10^{-1}
	0.1%	NaN	NaN	NaN	NaN	NaN	NaN	NaN	NaN	NaN	-4.40	2.08	1.23×10^{-2}
	1%	NaN	NaN	NaN	NaN	NaN	NaN	NaN	NaN	NaN	-7.20	1.89	7.45×10^{-4}
	10%	NaN	NaN	NaN	NaN	NaN	NaN	NaN	NaN	NaN	-10.32	1.03	3.31×10^{-5}
	100%	NaN	NaN	NaN	NaN	NaN	NaN	NaN	NaN	NaN	-12.70	3.39	3.04×10^{-6}
Pipe	0.01%	-11.73	0.72	8.02×10^{-6}	-11.73	0.72	8.02×10^{-6}	-7.93	0.99	3.61×10^{-4}	-12.84	1.32	2.67×10^{-6}
	0.1%	-12.51	0.71	3.70×10^{-6}	-12.51	0.71	3.70×10^{-6}	-9.68	0.79	6.24×10^{-5}	-13.45	1.43	1.44×10^{-6}
	1%	-13.86	1.25	9.56×10^{-7}	-13.86	1.25	9.56×10^{-7}	-11.43	1.51	1.08×10^{-5}	-14.06	1.16	7.85×10^{-7}
	10%	-14.59	1.19	4.61×10^{-7}	-14.59	1.19	4.61×10^{-7}	-13.20	1.29	1.85×10^{-6}	-14.67	1.36	4.25×10^{-7}
	100%	-15.74	1.85	1.47×10^{-7}	-15.74	1.85	1.47×10^{-7}	-14.94	2.11	3.25×10^{-7}	-15.29	1.83	2.30×10^{-7}
Valve	0.01%	-5.85	0.25	2.87×10^{-3}	-5.85	0.25	2.87×10^{-3}	-4.46	1.03	1.16×10^{-2}	-9.38	0.72	8.42×10^{-5}
	0.1%	-7.44	0.43	5.86×10^{-4}	-7.44	0.43	5.86×10^{-4}	-6.26	0.83	1.91×10^{-3}	-10.08	0.98	4.20×10^{-5}
	1%	-9.82	1.14	5.44×10^{-5}	-9.82	1.14	5.44×10^{-5}	-8.07	1.54	3.14×10^{-4}	-10.74	1.15	2.17×10^{-5}
	10%	-10.61	0.63	2.47×10^{-5}	-10.61	0.63	2.47×10^{-5}	-9.85	0.65	5.27×10^{-5}	-11.34	1.94	1.19×10^{-5}
	100%	-12.24	1.37	4.82×10^{-6}	-12.24	1.37	4.82×10^{-6}	-11.67	1.43	8.51×10^{-6}	-11.95	1.93	6.46×10^{-6}
Vaporizer	0.01%	NaN	NaN	NaN	NaN	NaN	NaN	NaN	NaN	NaN	-4.82	2.55	8.08×10^{-3}
	0.1%	NaN	NaN	NaN	NaN	NaN	NaN	NaN	NaN	NaN	-3.65	1.87	2.61×10^{-2}
	1%	NaN	NaN	NaN	NaN	NaN	NaN	NaN	NaN	NaN	-2.48	1.22	8.41×10^{-2}
	10%	NaN	NaN	NaN	NaN	NaN	NaN	NaN	NaN	NaN	-1.30	0.71	2.72×10^{-1}
	100%	NaN	NaN	NaN	NaN	NaN	NaN	NaN	NaN	NaN	-0.13	0.71	8.76×10^{-1}
Vessel	0.01%	NaN	NaN	NaN	-7.34	1.78	6.47×10^{-4}	NaN	NaN	NaN	-7.64	1.15	4.79×10^{-4}
	0.1%	NaN	NaN	NaN	-8.89	2.55	1.38×10^{-4}	NaN	NaN	NaN	-8.88	2.22	1.39×10^{-4}
	1%	NaN	NaN	NaN	-10.47	2.05	2.82×10^{-5}	NaN	NaN	NaN	-10.15	1.92	3.91×10^{-5}
	10%	NaN	NaN	NaN	-12.08	2.73	5.66×10^{-6}	NaN	NaN	NaN	-11.42	2.42	1.10×10^{-5}
	100%	NaN	NaN	NaN	-13.66	3.13	1.17×10^{-6}	NaN	NaN	NaN	-12.70	3.18	3.05×10^{-6}

2.4.3. Frequency of Dispenser Releases

The annual frequency of other releases ($f_{\text{Other Releases}}$) deals with failures that can happen at a dispenser, rather than random leaks from individual components. In addition to random leaks that can develop from any component at any time, there is also the possibility of a release occurring due to some component failure or accident while fueling. The probability of an accident can be high for several reasons: fueling typically involves direct human interaction to operate the fueling dispenser, involves temporary connections rather than hard-plumbed lines, and the connection could be inadvertently broken because the vehicle is not a permanent part of the system. On the other hand, releases from fueling can only occur when fueling occurs, and so different systems that involve different number of fueling events can be impacted by these releases to varying degrees. It is assumed that a dispenser failure would result in a large release of fuel, and so this frequency is only used in the largest (100%) leak size. The annual frequency of other releases ($f_{\text{Other Releases}}$) is calculated by the following equation:

$$f_{\text{Other Releases}} = f_{\text{Fueling Demands}} \times P(\text{Dispenser Releases}) \tag{16}$$

where $f_{\text{Fueling Demands}}$ is the annual frequency of fueling demands (i.e., the number of times a dispenser is used to refuel a vehicle in a year) and $P(\text{Dispenser Releases})$ is the probability of a release from a dispenser during fueling. The annual frequency of fueling demands is given by:

$$f_{\text{Fueling Demands}} = N_{\text{Vehicles}} \times N_{\text{Fuelings per Day}} \times N_{\text{Operating Days per Year}} \tag{17}$$

where N_{Vehicles} is the number of vehicles at the facility, $N_{\text{Fuelings per Day}}$ is the average number of times each vehicle is fueled per day, and $N_{\text{Operating Days per Year}}$ is the number of operating days in a year.

Dispenser failures are categorized in HyRAM+ as Accidents (in which the vehicle tank overpressurizes or a drive-off occurs) or Shutdown Failures (in which the system failures to shut down after a release from the nozzle). The probability for these types of releases are determined by a fault tree as shown in Figure 2-5.

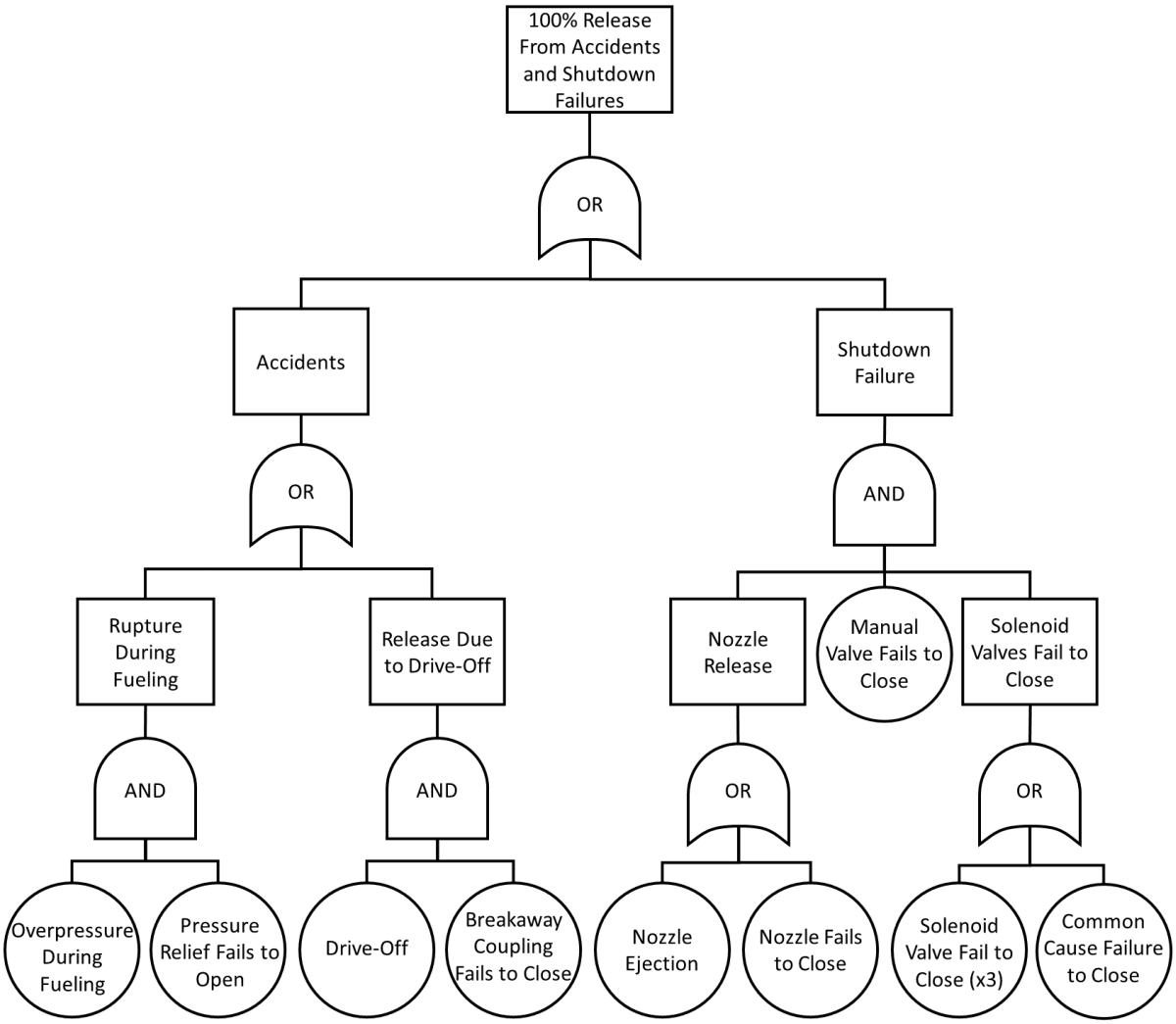

Figure 2-5 Fault Tree for Other Releases from a Dispenser

The probability of a release from a dispenser during fueling is given by:

$$P(\text{Dispenser Releases}) = P(\text{Accidents}) + P(\text{Shutdown Failure}) \tag{18}$$

where $P(\text{Accidents})$ is the probability of an accident during fueling and $P(\text{Shutdown Failure})$ is the probability of a shutdown failure during fueling. The probability of an accident during fueling is given by:

$$P(\text{Accidents}) = P(\text{Rupture During Fueling}) + P(\text{Release Due to DriveOff}) \tag{19}$$

where $P(\text{Rupture During Fueling})$ is the probability of a rupture that occurs during fueling and $P(\text{Release Due to DriveOff})$ is the probability of a release occuring due to a vehicle drive-off. The probability of a rupture that occurs during fueling is given by:

$$P(\text{Rupture During Fueling}) = P(\text{Overpressure During Fueling}) \times P(\text{PRD FTO}) \quad (20)$$

where P(Overpressure During Fueling) is the probability of an overpressure occuring during fueling (e.g., the dispenser over-fills the vehicle tank) and P(PRD FTO) is the probability of the dispenser pressure relief device failing to open on demand. The probabilities P(Overpressure During Fueling) and P(PRD FTO) can each be specified as a specific expected value from 0.0 to 1.0, or can be specified as a probability distribution such as Beta or Log-Normal distributions. If a probability distribution is specified, the mean value will be calculated and used in the above calculations. Default values for these probabilities are given in Section 2.4.4.

The probability of a release occuring due to a vehicle drive-off is given by:

$$P(\text{Release Due to DriveOff}) = P(\text{DriveOff}) \times P(\text{Breakaway FTC}) \quad (21)$$

where P(DriveOff) is the probability of a vehicle driving off while still attached to the dispenser during fueling and P(Breakaway FTC) is the probability of the breakaway coupling failing to close on demand. The probabilities P(DriveOff) and P(Breakaway FTC) can each be specified as a specific expected value from 0.0 to 1.0, or can be specified as a probability distribution such as Beta or Log-Normal distributions. If a probability distribution is specified, the mean value will be calculated and used in the above calculations. Default values for these probabilities are given in Section 2.4.4.

The probability of a shutdown failure during fueling is given by:

$$P(\text{Shutdown Failure}) = P(\text{Nozzle Release}) \times P(\text{Manual Valve FTC}) \times P(\text{Solenoid Valves FTC}) \quad (22)$$

where P(Nozzle Release) is the probability of the dispensing nozzle releasing fuel, P(Manual Valve FTC) is the probability of the manual shutoff valve failing to close on demand, and P(Solenoid Valves FTC) is the probability of the automated solenoid valves on the dispenser failing to close on demand. The probability of the manual shutoff valve failing to close on demand (P(Manual Valve FTC)) can be specified as a specific expected value or can be specified as a probability distribution (Beta or Log-Normal) for which the mean value will be used. Default values for this probability are given in Section 2.4.4.

The probability of the dispensing nozzle releasing fuel is given by:

$$P(\text{Nozzle Release}) = P(\text{Nozzle Ejection}) + P(\text{Nozzle FTC}) \quad (23)$$

where P(Nozzle Ejection) is the probability of the dispenser nozzle being ejected during fueling, and P(Nozzle FTC) is the probability of the dispenser nozzle failing to close on demand. These probabilities P(Nozzle Ejection) and P(Nozzle FTC) can each be specified as a specific expected value or can be specified as a probability distribution (Beta or Log-Normal) for which the mean value will be used. Default values for this probability are given in Section 2.4.4.

The probability of the automated solenoid valves on the dispenser failing to close on demand is given by:

$$P(\text{Solenoid Valves FTC}) = [P(\text{Solenoid Valve FTC})]^3 + P(\text{Common Cause FTC}) \tag{24}$$

where $P(\text{Solenoid Valve FTC})$ is the probability of any one automated solenoid valve failing to close on demand and $P(\text{Common Cause FTC})$ is the probability of something causing all of the solenoid valves to fail to close on demand (e.g., loss of connection to sensors). It should be noted that this fault tree assumes that there are 3 solenoid valves and that all of them need to fail in order for fuel to be released; thus, the probability for any single valve is cubed. These probabilities $P(\text{Solenoid Valve FTC})$ and $P(\text{Common Cause FTC})$ can each be specified as a specific expected value or can be specified as a probability distribution (Beta or Log-Normal) for which the mean value will be used. Default values for this probability are given in Section 2.4.4.

It should be noted that any of the probabilities in this section can be used to estimate an annual frequency of how often any of the events in question are expected to happen in a year. This can be done by multiplying the probability of interest ($P(A)$) by the annual number of fueling demands ($f_{\text{Fueling Demands}}$) for some event A:

$$f_A = P(A) \times f_{\text{Fueling Demands}} \tag{25}$$

2.4.4. Default Dispenser Failure Probabilities

In HyRAM+ 4.0, only the geometric mean (median) leak frequency is used in release calculations for the lognormal distributions and the arithmetic mean is used for the beta distributions. Future versions of HyRAM+ may be designed to use additional information from these distributions in uncertainty propagation.

See Section 2.4.2 for the calculation of the geometric mean for a lognormal distribution. For a beta distribution with parameters α and β, the arithmetic mean is given by:

$$\text{mean} = \frac{\alpha}{\alpha + \beta} \tag{26}$$

The default failure probabilities in this section were assembled from generic data from the offshore oil, process chemical, and nuclear power industries, and are taken directly from Ref [14].

Table 2-3 Default Probability Distributions for Component Failure

Component	Failure Mode	Distribution Type	Parameters
Nozzle	Pop-off	Beta (α, β)	$\alpha = 0.5$, $\beta = 610415.5$
Nozzle	Failure to close	Expected value	0.002
Breakaway coupling	Failure to close	Beta (α, β)	$\alpha = 0.5$, $\beta = 5031$
Pressure relief valve	Premature open	Beta (α, β)	$\alpha = 4.5$, $\beta = 310288.5$
Pressure relief valve	Failure to open	Lognormal (μ, σ)	$\mu = -11.74$, $\sigma = 0.67$
Manual valve	Failure to close (human error)	Expected value	0.001
Solenoid valve	Failure to close	Expected value	0.002
Solenoid valves	Common cause failure (3 valves, beta factor method)	Expected value	1.28×10^{-4}

Table 2-4 Default Probability Distributions for Accident Occurrence

Accident	Distribution Type	Parameters
Drive-off	Beta (α, β)	$\alpha = 31.5$, $\beta = 610384.5$
Overpressure during fueling	Beta (α, β)	$\alpha = 3.5$, $\beta = 310289.5$

2.5. Consequence Models

2.5.1. Facility Occupants

The harm and fatalities of interest in HyRAM+ are assumed to happen to facility occupants. Risk contours or risk at a specific location (such as a building or lot line) are not calculated explicitly. The risk for the entire facility is a summation of fatality risk for each of the user-specified occupant locations.

The occupant positions and number of occupants are defined by user input. For each dimension (x, y, z) for each occupant, the user may assign a position deterministically or may use a probability distribution to be randomly sampled to assign the positions over a user-specified range defined by a uniform or normal probability distribution. The occupant positions are all defined as relative to the leak point; i.e., the leak occurs at the "origin" (0, 0, 0) and extends in the positive-x direction, so the occupant positions (x, y, z) are based on that point. The x and z coordinates are horizontal to the ground, while the y coordinate is height above the ground.

The physical hazardous effects of the leak are calculated for each occupant position. For leak scenarios in which a jet fire occurs (immediate ignition of the leak), the heat flux from a jet flame is the hazardous consequence of interest. For scenarios that result in an explosion (delayed ignition of the leak), the hazard of interest is the overpressure that would occur at the occupant location. These physical hazards are then used with the harm model facility probits (see Section 2.6) to estimate probable fatalities, which are then used in the risk metric calculations (see Section 2.2).

2.5.2. Jet Fire

The consequences of a jet fire (for each of the five release sizes) on facility occupants are calculated using the models described in Section 3. The flame model described in Section 3.4.2 and multi-point radiative heat flux model described in Section 3.4.3 are used. These models are coupled to the orifice flow and notional nozzle models described in Section 3.3. The discharge coefficient C_d is set to 1.0 for the QRA calculations. The heat flux calculation is performed at each of the occupant locations.

2.5.3. Overpressure

Users must input the peak overpressure and impulse values for the five release sizes. These values can come from calculations using computational simulation, first-order models, or engineering assumptions. These values are then applied to all facility occupants. Subsequent versions of HyRAM+ will improve the treatment of overpressure per occupant and will allow a way to estimate overpressure and impulse values directly in the QRA calculation, similar to how heat flux thermal hazards are estimated.

2.5.4. Default Overpressure and Impulse Values

Currently, HyRAM+ uses a set of peak overpressure and impulse values as the default for delayed ignition scenarios; these values are editable by the user. The peak overpressure and impulse are used with the overpressure harm models in Section 2.6.2. The default peak overpressure values given in HyRAM+ are taken from numerical simulations performed for a warehouse with hydrogen-powered forklifts [14]. These simulations calculated peak overpressure values for the 100%, 10%, and 1% leak sizes; the smaller leak sizes (0.1% and 0.01%) used half of the peak overpressure as the 1% leak size. Default values for impulse are taken from the same simulations [14], which estimated the impulse for the largest leak size (100%) and assumed that smaller leaks produce half of the impulse as the next-largest leak. The default peak overpressure and impulse values in HyRAM+ are given in Table 2-5.

Table 2-5 Peak Overpressure and Impulse Values

Leak Size	Peak Overpressure (Pa)	Impulse (Pa·s)
0.01%	2500	250
0.1%	2500	500
1%	5000	1000
10%	16000	2000
100%	30000	4000

2.6. Harm and Loss Models

Probit models are used to establish the probability of injury or fatality for a given exposure. The probit model is a linear combination of predictors that model the inverse cumulative distribution function associated with the normal distribution[6]. The probability of a fatality is given by Equation 27, which evaluates the normal cumulative distribution function, Φ, at the value established by the appropriate probit model (Y, see Sections 2.6.1 and 2.6.2).

$$P(\text{fatality}) = F(Y|\mu = 5, \sigma = 1) = \Phi(Y - 5) \tag{27}$$

2.6.1. Thermal Harm

For thermal radiation, the harm level is a function of both the heat flux intensity and the duration of exposure. Harm from radiant heat fluxes is often expressed in terms of a thermal dose unit (V) which combines the heat flux intensity and exposure time by Equation 28:

$$V = I^{(4/3)} \times t \tag{28}$$

where I is the radiant heat flux in W/m^2 and t is the exposure duration in seconds. The default thermal exposure time used in HyRAM+ is 60 s, but users may modify this value.

Table 2-6 lists five thermal probit models that are encoded in HyRAM+. The probability of a fatality is evaluated by inserting the probit model from Table 2-6 into Equation 27. LaChance et al. [20] recommend using both the Eisenberg and the Tsao & Perry probit models for hydrogen-related applications.

Table 2-6 Probit models used to calculate fatality probability as a function of thermal dose (V)

Reference	Fatality Model	Notes
Eisenberg [21]	$Y = -38.48 + 2.56 \times \ln(V)$	Based on population data from nuclear blasts at Hiroshima and Nagasaki (ultraviolet radiation)
Tsao & Perry [22]	$Y = -36.38 + 2.56 \times \ln(V)$	Eisenberg model, modified to account for infrared radiation
TNO [23]	$Y = -37.23 + 2.56 \times \ln(V)$	Tsao and Perry model modified to account for clothing
Lees [24]	$Y = -29.02 + 1.99 \times \ln(0.5V)$	Accounts for clothing, based on porcine skin experiments using ultraviolet source to determine skin damages. Uses burn mortality information.

[6]Today, probit model are associated with the standard normal distribution, with mean $\mu = 0$ and standard deviation $\sigma = 1$. Some older probit models were developed using $\mu = 5$ to avoid negative values. HyRAM+ uses $\mu = 5$ to be consistent with the published fatality probit models.

Structures and equipment can also be damaged by exposure to radiant heat flux. Some typical heat flux values and exposure times for damage to structures and components were provided by LaChance et al. [20]. However, because the exposure times required for damage is long (>30 min), the impact of thermal radiation from fires on structures and equipment is not generally significant since personnel are able to evacuate the building before significant structural damage occurs. This is only noted because structural damage can cause physical harm (fatalities) to humans, which is the risk metric of interest within HyRAM+.

2.6.2. Overpressure Harm

There are several probit models available to predict harm and loss from blast overpressures. These models generally differentiate between direct and indirect effects of pressure. Significant increases in pressure can cause damage to pressure-sensitive organs such as the lungs and ears. Indirect effects include the impact from fragments and debris generated by the overpressure event, collapse of structures, and heat radiation (e.g., from the fireball generated during a vapor cloud explosion). Large explosions can also carry a person some distance resulting in injury from collisions with structures or from the resulting violent movement. The probit models for the effects of overpressures that are included in HyRAM+ are provided in Table 2-7.

Table 2-7 Probit models to calculate fatality probability from exposure to overpressures, where P_s is peak overpressure (Pa) and i is the impulse of the shock wave (Pa·s)

Reference	Fatality Model
Eisenberg - Lung hemorrhage [2]	$Y = -77.1 + 6.91\ln(P_s)$
HSE - Lung hemorrhage [25, 26]	$Y = 5.13 + 1.37\ln(P_s \times 10^{-5})$
TNO - Head impact [23]	$Y = 5 - 8.49\ln[(2430/P_s) + 4.0 \times 10^8/(P_s i)]$
TNO - Structure collapse [23]	$Y = 5 - 0.22\ln[(40000/P_s)^{7.4} + (460/i)^{11.3}]$

LaChance et al. [20] recommend the use of the TNO probit models, and suggest that indirect effects from overpressure events represent the most important concern for people. The overpressures required to cause fatal lung damage are significantly higher than the values required to throw a person against obstacles or to generate missiles that can penetrate the skin. In addition, a person inside a structure would more likely be killed by the facility collapse than from lung damage. For this reason, the HyRAM+ default is the TNO probit model for structural collapse.

This page intentionally left blank.

3. PHYSICS MODELS

HyRAM+ includes a physics mode, which provides models relevant to the behavior, hazards, and consequences of releases of the different fuels. Jet flames, concentration profiles for unignited jets/plumes, overpressure from the delayed ignition of a plume, and indoor accumulation with delayed ignition causing overpressure can all be investigated from the physics mode. A subset of these models is used in the QRA mode to calculate the consequences from a given release scenario, as described in Section 2.5. Several basic property calculations (e.g., the thermodynamic equation of state) are necessary to numerically simulate the release scenarios, and these property calculations are used in other models.

3.1. Properties of the Fluids

The modules in this section provide thermodynamic properties of unignited and ignited hydrogen, methane, and propane, which are needed to calculate different aspects of dispersion and combustion. These calculations are called from several of the other models. They are described here in detail, and then referred to in subsequent sections.

3.1.1. Equation of State

Description: HyRAM+ 4.0 utilizes the CoolProp library [27], called through its Python interface to perform several thermodynamic calculations. The property calculations are based on a Helmholtz energy function, and account for the real gas behavior at high pressures and at liquid (which can be cryogenic) temperatures. CoolProp [27] can be used to calculate the properties of hydrogen, methane, propane, air or other gases. For hydrogen, the relationships and energy functions are detailed in Leachman et al. [28], for methane, in Setzmann and Wagner [29], and for propane, in Lemmon et al. [30]. These thermodynamic calculations are used to calculate leak rates and are used in mass, momentum, and energy balances in regions close to the leak point. As an example, for hydrogen, the relationships between pressure[7], temperature, density, enthalpy, and entropy are plotted in Figure 3-1. In some regions of the models, the ideal gas equation of state is used, as described in other sections.

[7] HyRAM+ calculation inputs use absolute pressure, not gauge pressure

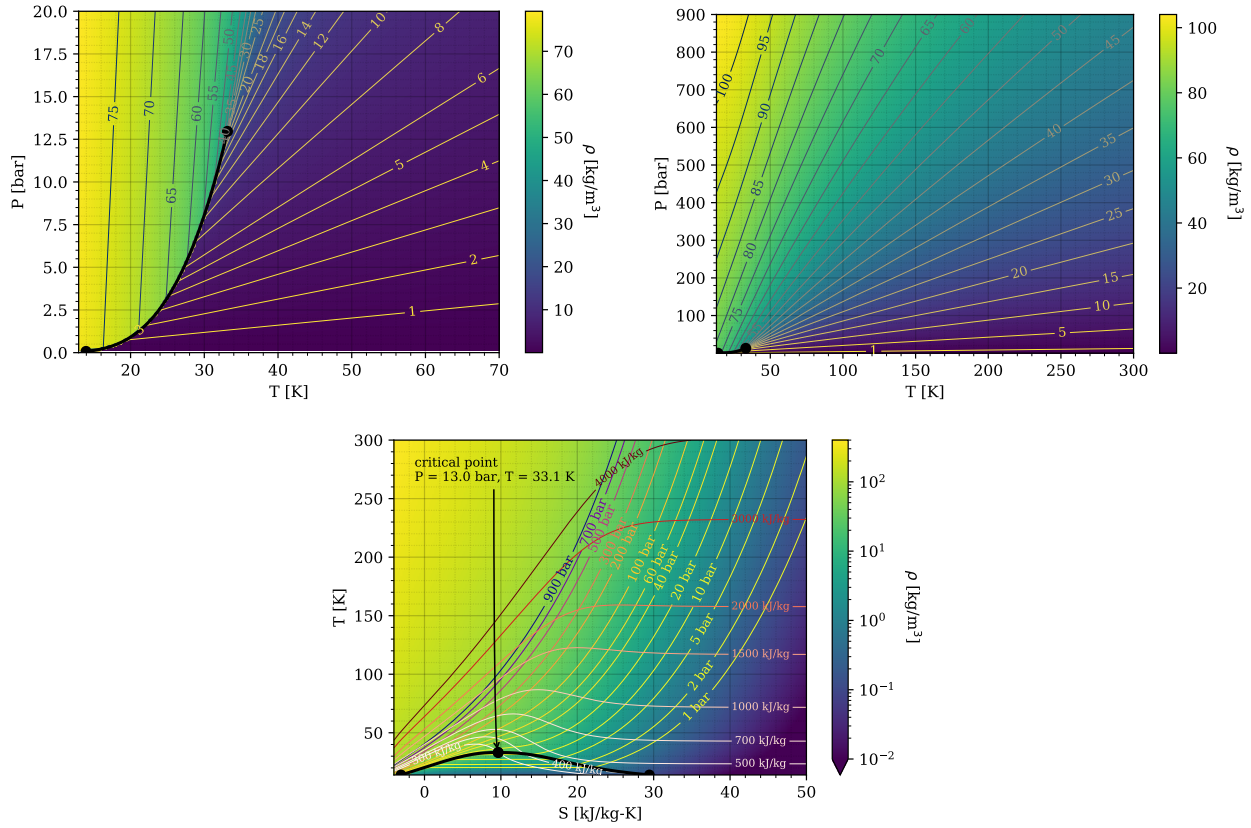

Figure 3-1 Graphical representations of state points, calculated using CoolProp [27] which is referencing the Leachman et al. [28] equation of state for hydrogen. Top plots show shading and iso-contours of density as a function of temperature and pressure. Bottom plot shows shading of density as a function of entropy and temperature, with iso-contours of pressure and enthalpy.

Applicability: The fundamental equation of state described by Leachman et al. [28] is valid for hydrogen at pressures up to 2000 MPa and between 14 K and 1000 K. The equation of state for methane described by Setzmann and Wagner [29] is valid from 90 K to 620 K at pressures up to 1000 MPa. The relationships described by Lemmon et al. [30] are valid for propane from from 85.5 K to 650 K and for pressures up to 1000 MPa. Note that HyRAM+ can often calculate outputs for temperatures and pressures outside the range of validity.

3.1.2. Combustion

Description: HyRAM+ flame calculations are based on the work of Ekoto et al. [31] and rely on several underlying properties of burned fuel, namely the stoichiometric mixture fraction, f_s, the heat of combustion, ΔH_c, along with the temperature, molecular weight and density of combustion products for a given mixture fraction, which is conserved during combustion.

Assumptions: Combustion is only assumed to occur in expanded fuel at atmospheric pressure. The ideal gas equation is used to calculate the density of the product mixture (ρ) based on the molecular weight of the mixture ($MW_{mixture}$), the temperature (T), and the gas constant (R):

$$\rho = \frac{P(\mathrm{MW_{mixture}})}{RT} \tag{29}$$

These combustion calculations assume that there are no losses, that the mixture is thermally perfect with the local enthalpy, and the pressure of the products is the same as the pressure of the reactants.

Relationships: Stoichiometric combustion of a fuel in air (ignoring the minor species in air) can be written as

$$\mathrm{C_nH_{2n+2}} + \frac{3\mathrm{n}+1}{2}(\mathrm{O_2} + 3.76\mathrm{N_2}) \rightarrow (\mathrm{n}+1)\mathrm{H_2O_{(g)}} + \mathrm{nCO_2} + 1.88(3\mathrm{n}+1)\mathrm{N_2} \tag{30}$$

During combustion, 242 kJ is released for every mole of gaseous water produced, and 394 kJ is released for every mole of carbon dioxide produced [32]. Therefore, when $n = 0$ and hydrogen is the fuel, the heat of combustion is 242 $\mathrm{kJ/mol_{H_2}}$ or 120 $\mathrm{MJ/kg_{H_2}}$ (using the lower heating value) [33, 34]. For methane and propane, the heats of combustion are 50 MJ/kg and 46.4 MJ/kg, respectively. From Eq. 30, the stoichiometric mixture fraction (f_s), which is the same as the mass fraction of fuel, can be calculated as:

$$f_s = \frac{\mathrm{MW_{C_nH_{2n+2}}}}{\mathrm{MW_{C_nH_{2n+2}}} + \frac{3\mathrm{n}+1}{2}(\mathrm{MW_{O_2}} + 3.76\mathrm{MW_{N_2}})} \tag{31}$$

The stoichiometric mixture fractions for hydrogen, methane, and propane are 0.02852, 0.05519, and 0.06034 respectively. If incomplete combustion occurs (a mixture fraction other than stoichiometric), there will be excess air or fuel on the right hand side of Equation 30 at the temperature of the product stream. In other words,

$$\begin{aligned}\mathrm{C_nH_{2n+2}} + \eta\frac{3n+1}{2}(\mathrm{O_2} + 3.76\mathrm{N_2}) \rightarrow\ & \max(0, 1-\eta)\mathrm{C_nH_{2n+2}} + \\ & \min(1, \eta(n+1))\mathrm{H_2O} + \min(1, \eta n)\mathrm{CO_2} \\ & \max\left(0, (\eta-1)\frac{3n+1}{2}\right)\mathrm{O_2} + 3.76\eta\frac{3n+1}{2}\mathrm{N_2},\end{aligned} \tag{32}$$

where η, which specifies the mole fraction of air, can vary from 0 to ∞. In this case, the mixture fraction is equal to

$$f = Y_{\mathrm{C_nH_{2n+2}}} + Y_{\mathrm{H_2O}}\frac{\mathrm{MW_{C_nH_{2n+2}}}}{\mathrm{MW_{H_2O}}} + Y_{\mathrm{CO_2}}\frac{\mathrm{MW_{C_nH_{2n+2}}}}{\mathrm{MW_{CO2}}} \tag{33}$$

where Y is the mass fraction of products or reactants. HyRAM+ uses CoolProp [27] to calculate the enthalpy of H_2, H_2O, CO_2, O_2, and N_2 as a function of temperature and then solves for the temperature of products assuming an isenthalpic reaction, i.e.,

$$\sum_{i=\mathrm{C_nH_{2n+2}},\mathrm{O_2},\mathrm{N_2}} Y_{i,\mathrm{reac}} h_{i,\mathrm{reac}}(T_{\mathrm{reac}}, P_{\mathrm{reac}}) = \sum_{i=\mathrm{C_nH_{2n+2}},\mathrm{O_2},\mathrm{N_2},\mathrm{H_2O}} Y_{i,\mathrm{prod}} h_{i,\mathrm{prod}}(T_{\mathrm{prod}}, P_{\mathrm{prod}}) + Y_{\mathrm{H_2O,prod}} \frac{\mathrm{MW_{C_nH_{2n+2}}}}{(\mathrm{n}+1)\mathrm{MW_{H_2O}}} \Delta H_c \tag{34}$$

The calculation of the adiabatic flame temperature (T_{ad}) and density of the products of 298 K, 101,325 Pa fuels are shown in Figure 3-2.

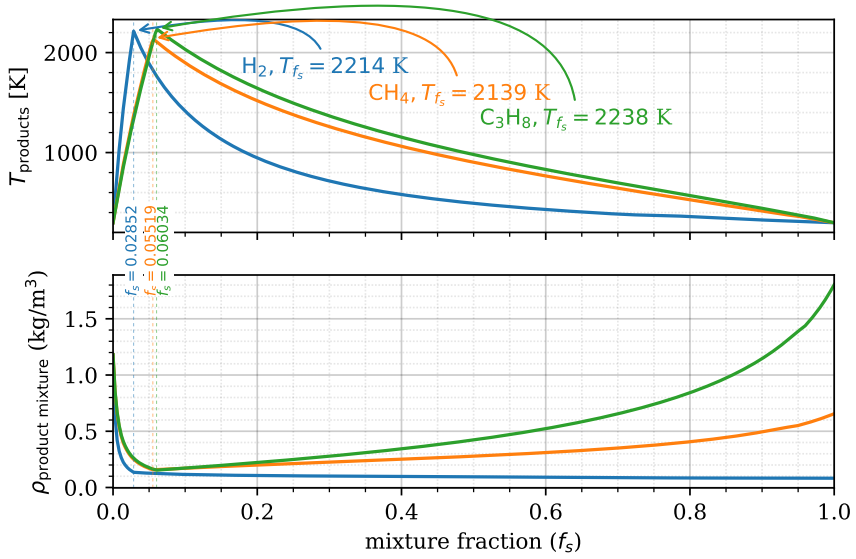

Figure 3-2 Temperature and density of products for the combustion of 298 K, 101,325 Pa fuels as a function of mixture fraction

Applicability: These combustion calculations are applicable in atmospheric pressure regions where heat losses are negligible.

3.2. Developing Flow

Several engineering models are used in HyRAM+ to establish the flow through an orifice, expand to atmospheric pressure, warm to a level that the equation of state is valid, and develop into the Gaussian profiles that are well known for jet/plume dispersion or diffusion flames.

3.2.1. Orifice Flow

HyRAM+ assumes that fluids flow isentropically through an orifice. CoolProp [27] is used to calculate the entropy (s_0) and enthalpy (h_0) of the fluid upstream of an orifice, using the specified pressure and temperature (or phase if a saturated vapor or saturated liquid is specified). CoolProp [27] is then used to calculate the enthalpy (h), temperature (T), and sonic velocity (a) of a fluid at atmospheric pressure with the same entropy as the upstream fluid (s_0). An isenthalpic expansion would require:

$$\frac{v^2}{2} + h = h_0 \tag{35}$$

but if the velocity, v, is faster than the speed of sound (a), the flow chokes, meaning that it is sonic (flowing at the speed of sound) through the orifice, but remains at a higher pressure than the atmospheric pressure. If $v = \sqrt{2(h_0 - h)} \leq a$, the calculation is finished and the fluid at the orifice is at atmospheric pressure and temperature (T), with a velocity of v. If $v = \sqrt{2(h_0 - h)} > a$, HyRAM+ will solve for the conditions (T and P) at the orifice such that

$$\begin{cases} s(T,P) = s_0 \\ \frac{a(s_0,P)^2}{2} + h(s_0,P) = h_0 \end{cases} \tag{36}$$

where $s(T,P)$ is the entropy at the orifice. In the case of choked flow, when the solution to the system of equations in 36 is satisfied, the calculation is finished and the fluid at the orifice is at pressure P, temperature T, and has a velocity of a, the speed of sound.

CoolProp [27] has well-defined routines for calculating the speed of sound of pure liquids and gases. In the two-phase region, there are various methods for calculating the speed of sound and depending on the version used, CoolProp [27] may not return a finite number for the speed of sound. HyRAM+ calculates the speed of sound for a two-phase mixture following the work of Chung et al. [35],

$$a = \frac{a_g a_l \sqrt{\frac{\rho_g a_g^2}{\alpha_l \rho_g a_g^2 + \alpha_g \rho_l a_l^2}}}{\alpha_l a_g + \alpha_g a_l \sqrt{\frac{\rho_g a_g^2}{\alpha_l \rho_g a_g^2 + \alpha_g \rho_l a_l^2}}} \tag{37}$$

where the subscript g is for the pure gas at the saturation point, the subscript l is for the pure liquid at the saturation point, and α is the volume fraction. The gas and liquid volume fractions add to 1.0, and the volume fraction of gas is calculated from the quality (Q) and density of the two-phase mixture (which are returned by CoolProp),

$$\alpha_g = Q\frac{\rho}{\rho_g} \tag{38}$$

Orifices in HyRAM+ are assumed to be circular, characterized by their diameter, d, and a coefficient of discharge, C_d. When the velocity and density of the fluid at the orifice is known, the mass flow rate is calculated as:

$$\dot{m} = \frac{\pi}{4} d^2 \rho v C_d \tag{39}$$

3.2.2. Notional Nozzles

Notional nozzles are used to calculate the effective diameter, velocity, and thermodynamic state after the complex shock structure of an under-expanded jet. In HyRAM+, a notional nozzle model is used if the pressure at the orifice is above atmospheric pressure. They are not necessarily a physical description of the phenomena, but a jet with the diameter, velocity and state (temperature and atmospheric pressure) of the notional nozzle would lead to the same dispersion characteristics as the underexpanded jet. There are five different notional nozzle models in HyRAM+, with each model conserving mass between flow through the real orifice and flow through the notional nozzle. This means that

$$\rho_{\text{eff}} v_{\text{eff}} A_{\text{eff}} = \rho_{\text{throat}} v_{\text{throat}} A_{\text{throat}} C_D \tag{40}$$

where ρ is the density, v is the velocity, A is the cross-sectional area, C_D is the discharge coefficient, the subscript "throat" denotes the choke point (at the orifice, see Section 3.2.1), and the subscript "eff" denotes effective (after the shock structure and the pressure has returned to atmospheric).

The default notional nozzle model in HyRAM+ is based on the work of Yüceil and Ötügen [36]. In this case, mass (Equation 40), momentum, and energy are conserved. Conservation of momentum is written as

$$\rho_{\text{eff}} v_{\text{eff}}^2 A_{\text{eff}} = \rho_{\text{throat}} v_{\text{throat}}^2 A_{\text{throat}} C_D + A_{\text{throat}} (P_{\text{throat}} - P_{\text{ambient}}) \tag{41}$$

where P is the pressure. Simultaneous solution of Equations 40 and 41 yields a solution for the velocity at the notional nozzle

$$v_{\text{eff}} = v_{\text{throat}} C_D + \frac{P_{\text{throat}} - P_{\text{ambient}}}{\rho_{\text{throat}} v_{\text{throat}} C_D} \tag{42}$$

and the effective area of the notional nozzle

$$A_{\text{eff}} = \frac{\rho_{\text{throat}} v_{\text{throat}}^2 A_{\text{throat}} C_D^2}{\rho_{\text{eff}} \left(P_{\text{throat}} - P_{\text{ambient}} + \rho_{\text{throat}} V_{\text{throat}}^2 C_D^2 \right)} \tag{43}$$

Close examination of Equation 43 shows that the area calculation requires the effective density. The density is calculated using the conservation of energy (assuming isentropic expansion), where

$$\frac{v_{\text{eff}}^2}{2} + h(\rho_{\text{eff}}, P_{\text{ambient}}) = \frac{v_{\text{throat}}^2}{2} + h_{\text{throat}} \tag{44}$$

CoolProp [27] is used to calculate the enthalpy and Equation 44 is solved to determine the effective density.

Alternative to using Equation 44, Birch et al. (1987) [37] finds the effective density by assuming that the temperature of the notional nozzle is the same as the temperature of the stagnant gas, or

$$\rho_{\text{eff}} = \rho(T_0, P_{\text{ambient}}) \tag{45}$$

where T_0 is the temperature of the stagnant gas (storage temperature) and CoolProp [27] is used to calculate the density.

Three of the notional nozzle models do not conserve momentum, but rather assume that the notional nozzle velocity is at the speed of sound.

Following the work of Birch et al. (1984) [38], assuming that the temperature at the notional nozzle is the same as temperature of the stagnant gas, the density (see Equation 45) and velocity at the notional nozzle can be calculated

$$v_{\text{eff}} = a(T_0, P_{\text{ambient}}) \tag{46}$$

where a is the speed of sound, calculated using CoolProp [27] (see Equation 37). The conservation of mass, Equation 40, along with Equations 45 and 46, can be used to specify the notional nozzle conditions.

Alternatively, Ewan and Moody [39] use the assumption that the temperature at the notional nozzle is the same as the temperature at the throat, or

$$\rho_{\text{eff}} = \rho(T_{\text{throat}}, P_{\text{ambient}}) \tag{47}$$
$$v_{\text{eff}} = a(T_{\text{throat}}, P_{\text{ambient}}) \tag{48}$$

Finally, Molkov et al. [40] specifies that mass and energy are conserved between the orifice and the notional nozzle and that the notional nozzle is at the speed of sound, i.e., Equation 40 along with the simultaneous solution of the equations,

$$\frac{v_{\text{eff}}^2}{2} + h(\rho_{\text{eff}}, P_{\text{ambient}}) = \frac{v_{\text{throat}}^2}{2} + h_{\text{throat}} \tag{49}$$
$$v_{\text{eff}} = a(\rho_{\text{eff}}, P_{\text{ambient}}) \tag{50}$$

where h and a are calculated using CoolProp [27] (see Equation 37 regarding the speed of sound).

To summarize, the 5 different notional nozzles available in HyRAM+ solve the equations:

- (default) Yüceil and Ötügen [36]: Equations 42, 43, and 44
- Birch et al. (1987) [37]: Equations 42, 43, and 45
- Birch et al. (1984) [38]: Equations 40, 45, and 46
- Ewan and Moody [39]: Equations 40, 47, and 48
- Molkov et al. [40]: Equations 40, 49, and 50

3.2.3. Initial Entrainment and Heating

The models in HyRAM+ are valid for hydrogen, methane and propane, including saturated vapor and saturated liquid releases. Specifically for cryogenic hydrogen, as noted by Houf and Winters [41], there are challenges calculating properties in regions of the flow where oxygen and nitrogen from the entrained air would condense due to the extremely low temperatures. To account for this, conservation of mass, energy and momentum are applied until the temperature of the mixture (still assumed to be a plug-flow) is above a user specified temperature (T_{min}). If the temperature of the notional nozzle (or at the orifice, if the flow is unchoked) is below T_{min}, the state after initial entrainment and heating is specified as hydrogen at T_{min}, and simultaneous solution to the momentum and energy balances yields the mass fraction of hydrogen (Y) when the mixture has warmed to T_{min}, i.e.,

$$\dot{m}_{\text{out}} = \dot{m}_{\text{in}} + \frac{1-Y}{Y}\dot{m}_{\text{in}} \tag{51}$$

$$v_{\text{out}} = v_{\text{in}}\frac{\dot{m}_{\text{in}}}{\dot{m}_{\text{out}}} \tag{52}$$

$$h_{\text{out}} = (1-Y)h_{\text{air}}(T_{min}, P_{\text{ambient}}) + Y h_{\text{H}_2}(T_{min}, P_{\text{ambient}}) + \frac{v_{\text{out}}^2}{2} \tag{53}$$

$$\dot{m}_{\text{out}}h_{\text{out}} = \dot{m}_{in}h_{\text{in}} + (\dot{m}_{\text{out}} - \dot{m}_{\text{in}})h_{\text{air}}(T_{\text{ambient}}, P_{\text{ambient}}) \tag{54}$$

Once the mass fraction (Y) is known, conservation of mass is used to yield the diameter of the plug flow at the end of the zone of initial entrainment and heating,

$$\rho_{\text{out}} = \frac{1}{\frac{1-Y}{\rho_{\text{air}}(T_{min}, P_{\text{ambient}})} + \frac{Y}{\rho_{\text{H}_2}(T_{min}, P_{\text{ambient}})}} \tag{55}$$

$$d_{\text{out}} = \sqrt{\frac{\pi\dot{m}_{\text{out}}}{4\rho_{\text{out}}v_{\text{out}}}} \tag{56}$$

and the momentum driven entrainment rate (see Equation 78) is used to calculate the length of this zone,

$$S = \frac{(1-Y)(\dot{m}_{\text{out}} - \dot{m}_{\text{in}})}{\rho_{\text{ambient}}(T_{\text{ambient}}, P_{\text{ambient}})E_{mom}} \tag{57}$$

3.2.4. Establishment of a Gaussian Profile

The flows described in Sections 3.2.1, 3.2.2, and 3.2.3 are all assumed to be plug flows, where the properties (e.g., velocity, density) are constant across the entire cross-section of the flow. However, jets, plumes, or flames from a pure source are well-known to have Gaussian profiles of their properties (e.g., velocity, density, mixture fraction) in the downstream regions. The final model for developing flow describes the transition from plug flow to the Gaussian profile that is used as an input to a one-dimensional system of ordinary differential equations that describes unignited dispersion or a diffusion flame (see Sections 3.3 and 3.4.2). Following the work of Winters [42], the centerline velocity of the Gaussian flow is assumed to be equivalent to the plug

flow velocity, the jet is characterized by a half-width, B, where the velocity drops to half of the center-line value, and a spreading ratio, λ, the ratio of density spreading relative to velocity. The center-line (denoted with a cl subscript) mass-fraction is related to λ via the relationship,

$$\frac{\lambda^2+1}{2\lambda^2} = \frac{Y_{cl} - Y_{\text{ambient}}}{Y_{\text{plug}} - Y_{\text{ambient}}} \tag{58}$$

Then the center-line molecular weight can be calculated,

$$\text{MW}_{cl} = \frac{1}{Y_{cl}/\text{MW}_{\text{C}_\text{n}\text{H}_{2\text{n}+2}} + (1-Y_{cl})/\text{MW}_{\text{air}}} \tag{59}$$

The heat capacity of the fluid and ambient air are determined from CoolProp [27] and used to calculate the individual and mixture enthalpies as $h = c_p \cdot T$, where

$$c_{p,\text{plug}} = c_{p,\text{C}_\text{n}\text{H}_{2\text{n}+2}} Y_{\text{plug}} + c_{p,\text{air}}(1-Y_{\text{plug}}) \tag{60}$$

$$c_{p,cl} = c_{p,\text{plug}} Y_{cl} + c_{p,\text{air}}(1-Y_{cl}) \tag{61}$$

$$\frac{\lambda^2+1}{2\lambda^2} = \frac{h_{cl} - h_{\text{ambient}}}{h_{\text{plug}} - h_{\text{ambient}}} \tag{62}$$

From these equations, the center-line temperature can be calculated, and the center-line density is calculated using the ideal gas equation of state, where

$$\rho_{cl} = \frac{\text{MW}_{cl} P}{R T_{cl}} \tag{63}$$

The length of the developing flow region is taken from Abraham [43], where $S/d = 6.2$, which assumes that the Froude number (Eq. 82) is greater than the square root of 40 for these high speed, low density jets.

3.3. Unignited Releases

3.3.1. Gas Jet/Plume

For a jet or plume, HyRAM+ follows the one-dimensional model described by Houf and Winters [41]. While the model only considers one dimension, this dimension is along the streamline, and the jet/plume can curve due to buoyancy effects (or wind, although this aspect is not currently included). The reduction in dimension comes from the assumption that the mean

profiles of the velocity (v), density (ρ), and product of density and mass fraction (Y) of fuel are Gaussian, as

$$v = v_{cl} \exp\left(-\frac{r^2}{B^2}\right) \tag{64}$$

$$\rho = (\rho_{cl} - \rho_{amb}) \exp\left(-\frac{r^2}{\lambda^2 B^2}\right) + \rho_{amb} \tag{65}$$

$$\rho Y = \rho_{cl} Y_{cl} \exp\left(-\frac{r^2}{\lambda^2 B^2}\right) \tag{66}$$

where B is a characteristic half-width, λ is the ratio of density spreading relative to velocity, the subscript cl denotes the centerline, the subscript amb denotes ambient, and r is perpendicular to the stream-wise direction. Gravity acts in the negative y-direction, and the plume angle, θ is relative to the x-axis (horizontal), as shown in Figure 3-3.

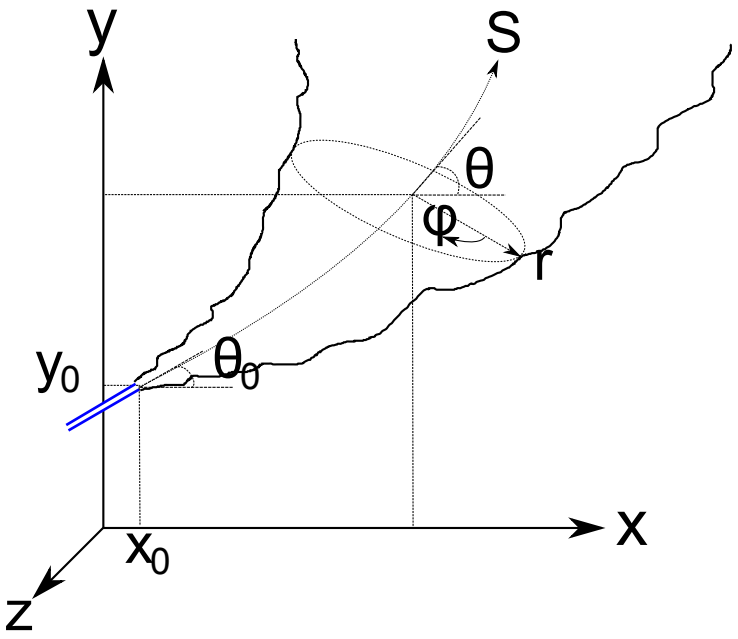

Figure 3-3 Sketch of plume model coordinates. Gravity acts in the negative y-direction

The derivatives of the spatial dimensions are therefore

$$\frac{dx}{dS} = \cos\theta \tag{67}$$

$$\frac{dy}{dS} = \sin\theta \tag{68}$$

The conservation equations can be written as follows:

continuity:

$$\frac{d}{dS}\int_0^\infty (\rho v) 2\pi r dr = \rho_{amb} E \tag{69}$$

x-momentum:

$$\frac{d}{dS}\int_0^\infty \left(\rho v^2 \cos\theta\right) 2\pi r dr = 0 \tag{70}$$

y-momentum:

$$\frac{d}{dS}\int_0^\infty \left(\rho v^2 \sin\theta\right) r dr = \int_0^\infty (\rho_{amb} - \rho) g r dr \tag{71}$$

species continuity:

$$\frac{d}{dS}\int_0^\infty (\rho v Y)\, 2\pi r dr = 0 \tag{72}$$

energy:

$$\frac{d}{dS}\int_0^\infty \rho v \left(h + \frac{v^2}{2} - h_{amb}\right) 2\pi r dr = 0 \tag{73}$$

Similar to Houf and Winters [41], HyRAM+ assumes that $h = c_p T$ and use the ideal gas equation of state for these ambient pressure mixtures. The mixture molecular weight, heat capacity, and product of density and enthalpy all vary with respect to the radial coordinate (due to the fact that Y and ρ vary radially, see Eq. 66) according to the following expressions:

$$\mathrm{MW} = \frac{\mathrm{MW}_{amb}\mathrm{MW}_{\mathrm{C}_n\mathrm{H}_{2n+2}}}{Y(\mathrm{MW}_{amb} - \mathrm{MW}_{\mathrm{C}_n\mathrm{H}_{2n+2}}) + \mathrm{MW}_{\mathrm{C}_n\mathrm{H}_{2n+2}}} \tag{74}$$

$$c_p = Y(c_{p,\mathrm{C_nH_{2n+2}}} - c_{p,amb}) + c_{p,amb} \tag{75}$$

$$\rho h = \frac{P}{c_p \mathrm{MW}} \tag{76}$$

The Gaussian profiles in Equations 64-66 are plugged into the governing equations, and with the exception of the energy equation can be integrated analytically. For the energy equation, Equation 73, the numeric integration to infinity is only evaluated to $5B$. This results in a system of 7 first order differential equations where the independent variable is S and the dependent variables are v_{cl}, B, ρ_{cl}, Y_{cl}, θ, x, and y. This system of equations is integrated from the starting point to the distance desired using an explicit Runge-Kutta method of order (4)5.

The entrainment model follows Houf and Schefer [44], where there is a combination of momentum and buoyancy driven entrainment,

$$E = E_{mom} + E_{buoy} \tag{77}$$

where

$$E_{mom} = 0.282 \left(\frac{\pi d_{\text{exp}}^2}{4} \frac{\rho_{\text{exp}} v_{\text{exp}}^2}{\rho_\infty} \right)^{1/2} \tag{78}$$

where the "exp" subscript denotes after the notional nozzle and zone of initial entrainment and heating (if used; see Sections 3.2.2 and 3.2.3), and

$$E_{buoy} = \frac{a}{\text{Fr}_l} (2\pi v_{cl} B) \sin\theta \tag{79}$$

where the local Froude number,

$$\text{Fr}_l = \frac{v_{cl}^2}{gD(\rho_\infty - \rho_{cl})/\rho_{\text{exit}}} \tag{80}$$

In these equations, a is empirically determined:

$$\begin{cases} a = 17.313 - 0.116665\text{Fr}_{\text{den}} + 2.0771 \times 10^{-4}\text{Fr}_{\text{den}}{}^2, & \text{Fr}_{\text{den}} < 268 \\ a = 0.97, & \text{Fr}_{\text{den}} \geq 268, \end{cases} \tag{81}$$

with the densimetric Froude number

$$\text{Fr}_{\text{den}} = \frac{v_{\text{plug}}}{\sqrt{g d_{\text{plug}} |\rho_\infty - \rho_{\text{plug}}| / \rho_{\text{plug}}}}, \tag{82}$$

where the subscript plug denotes the plug flow at the exit of the orifice, notional nozzle, or zone of initial entrainment and heating, as applicable (see Sections 3.2.1, 3.2.2, and 3.2.3).

As the jet/plume becomes buoyancy-dominated (as opposed to momentum-dominated), the non-dimensional number

$$\alpha = \frac{E}{2\pi B v_{cl}} \tag{83}$$

will increase. When α reaches the limiting value of $\alpha = 0.082$, α is held constant and the entrainment value becomes:

$$E = 2\pi\alpha B v_{cl} = 0.164\pi B v_{cl} \tag{84}$$

3.3.2. Tank Emptying

In the case of a storage tank with a given volume, the transient process of the tank emptying can also be calculated by HyRAM+. In this case, energy and mass are conserved, following the work of Hosseini et al. [45]. The mass flow rate, $\dot{m}$ is calculated as described in Section 3.2.1, whether the flow is choked or not. Energy is conserved in the tank volume, where

$$\frac{du}{dt} = \frac{\dot{m}(h-u) + q}{m}, \tag{85}$$

where u and h are the specific energy and specific enthalpy (J/kg), respectively, of the fuel in the tank (calculated using CoolProp [27]), m is the mass of fuel in the tank (kg), and q is the heat flow into the tank (J/s, $q = 0$ if adiabatic). This equation and the equations describing the mass flow rate (which are functions of the pressure and temperature inside the tank) are integrated until the mass or pressure in the tank reaches the desired stopping point (e.g., the tank pressure reaches ambient).

3.3.3. Accumulation in Confined Areas/Enclosures

When a release occurs in an enclosure, a stratified mixture of fuel and air can accumulate. For hydrogen or methane, the accumulated mixture will be near the ceiling due to buoyancy.

The release inside an enclosure is assumed to come from some tank with a fixed volume. Therefore, the flow from the tank follows Section 3.3.2. At each point in time for the blowdown, the jet/plume is modeled as described in Section 3.3.1. When these releases occur indoors, the plumes could impinge on a wall. Currently, should this impingement happen, the trajectory of the jet/plume is modified such that the fuel will travel vertically upwards along the wall, rather than in the horizontal direction, with the same features (e.g. half-width, centerline velocity). Note that this deflection upwards will occur regardless of the fuel and is a poor assumption for heavier fuels such as propane.

Accumulation occurs following the model of Lowesmith et al. [46], where a layer forms along the ceiling. Conservation of mass requires that

$$\frac{dV_l}{dt} = Q_{\text{in}} - Q_{\text{out}} \tag{86}$$

where V_l is the volume of gas in the layer, and Q is the volumetric flow rate, with subscript in referring to the flow rate of fuel and air entrained into the jet at the height of the layer, and out referring to flow out the ventilation. Species conservation requires that

$$\frac{d(\chi V_l)}{dt} = Q_{\text{leak}} - \chi Q_{\text{out}} \tag{87}$$

where χ is the mole or volume fraction of fuel in the layer and Q_{leak} is the leak rate of the fuel. Expanding the derivative and substituting Equation 86 yields

$$V_l \frac{d\chi}{dt} = Q_{\text{leak}} - \chi Q_{\text{in}} \tag{88}$$

Q_{in} is solved for by modeling a jet/plume within the enclosure to calculate the jet half-width (B) and centerline velocity (v_{cl}), as described in Section 3.3.1 at the height of the bottom of the layer. The volumetric flow rate (Q_{in}) is calculated as:

$$Q_{\text{in}} = \pi B^2 v_{cl} \tag{89}$$

Flows out of the enclosure are driven by buoyancy, and potentially wind or a fan. Buoyancy driven flow is calculated as

$$Q_B = C_d A_v \sqrt{g' H_l} \tag{90}$$

where C_d is a coefficient of discharge, A_v is the area of the upper (outlet) vent, H_l is the height of the layer (between the bottom of the layer and the center-point of the outlet vent), and g' is reduced gravity:

$$g' = g \frac{\rho_{\text{air}} - \rho_l}{\rho_{\text{air}}} \tag{91}$$

where g is the gravitational constant, ρ_l is the density of the layer, and ρ_{air} is the density of air (at the temperature and pressure of the enclosure). The density in the layer (ρ_l) is calculated from the density of air (ρ_{air}) and the density of the fuel ($\rho_{C_nH_{2n+2}}$), both at the temperature and pressure of the enclosure, as:

$$\rho_l = \chi\rho_{C_nH_{2n+2}} + (1-\chi)\rho_{\text{air}} \tag{92}$$

Wind (or mechanical ventilation) is assumed to drive the flow at a rate of:

$$Q_w = \frac{C_d A_v U_w}{\sqrt{2}} = \frac{C_d Q_{\text{vent}}}{\sqrt{2}} \tag{93}$$

where C_d is a coefficient of discharge, A_v is the area of the lower (inlet) vent, U_w is the velocity of the wind (or mechanical ventilation) through the lower (inlet) vent, and Q_{vent} is the volumetric flow rate through the lower (inlet) vent ($Q_{\text{vent}} = A_v U_w$). Note that Q_{vent} is a user input.

The total flow out of the enclosure is calculated as

$$Q_{\text{out}} = Q_{\text{leak}} + \sqrt{Q_b^2 + Q_w^2} \tag{94}$$

3.4. Ignited Releases

3.4.1. Flame Correlations

As noted by Houf and Schefer [47], a non-dimensional flame length, defined as

$$L^* = \frac{L_{\text{vis}} f_s}{d_j \sqrt{\rho_j / \rho_{amb}}} \tag{95}$$

collapses onto a single curve for a range of fuels (hydrogen, methane, and propane), where L_{vis} is the visible flame length, f_s is the mass fraction of fuel in a stoichiometric mixture of fuel and air (Equation 31), and d_j, ρ_j, and ρ_{amb} are the orifice diameter, density of fuel at the orifice, and density of air, respectively. The curve is given by

$$L^* = \begin{cases} \frac{13.5\text{Fr}^{2/5}}{(1+0.07\text{Fr}^2)^{1/5}}, & \text{Fr} < 5 \\ 23, & \text{Fr} > 5 \end{cases} \tag{96}$$

which is a function of the Froude number (Fr), which is the ratio of buoyancy to momentum forces. The Froude number is defined as

$$\text{Fr} = \frac{u_j f_s^{3/2}}{\sqrt{g d_j (T_{\text{ad}} - T_{amb})/T_{amb}} \sqrt{\rho_j / \rho_{amb}}} \tag{97}$$

where g is the gravitational constant, u_j is the velocity of the jet at the orifice, T_{ad} is the adiabatic flame temperature (for a stoichiometric mixture, see section 3.1.2), and T_{amb} is the ambient temperature. The flame width is constant at $W_f = 0.17 L_{\text{vis}}$ [48, 49].

The total emitted radiative power from a flame, S_{rad}, is related to the total energy in the flame by the radiant fraction,

$$S_{\text{rad}} = X_{\text{rad}} \dot{m}_{\text{fuel}} \Delta H_c \tag{98}$$

where X_{rad} is the radiant fraction, $\dot{m}_{\text{fuel}}$ is the mass flow rate of fuel, and ΔH_c is the heat of combustion (120 MJ/kg for hydrogen, 50 MJ/kg for methane, and 46.4 MJ/kg for propane [33, 34]). The radiant fraction (X_{rad}) varies with the flame residence time (τ_f); the relationship is [50]

$$X_{\text{rad}} = 9.45 \times 10^{-9} (\tau_f a_p T_{\text{ad}}^4)^{0.47} \tag{99}$$

where a_p is the Planck-mean absorption coefficient for an optically thin flame (0.23 for hydrogen [51]). The Plank-mean absorption coefficient should be updated for methane and propane, but the current value of 0.23 is used for all fuels. The flame residence time can be calculated as

$$\tau_f = \frac{\rho_f W_f^2 L_{\text{vis}} f_s}{3 \rho_j d_j^2 u_j} \tag{100}$$

where ρ_f is the flame density. The flame density is calculated as the density at the adiabatic flame temperature:

$$\rho_f = \frac{p_{amb} W_{\text{mix}}}{R T_{\text{ad}}} \tag{101}$$

where p_{amb} is the ambient pressure, W_{mix} is the mean molecular weight of the stoichiometric products of combustion in air, and R is the universal gas constant.

The transmissivity, which can reduce the radiated heat flux is calculated to account for the absorption from water vapor and CO_2, using a correlation from Wayne [52]:

$$\begin{aligned} \tau = 1.006 &- 0.001171 \left(\log_{10} X_{\text{H}_2\text{O}}\right) - 0.02368 \left(\log_{10} X_{\text{H}_2\text{O}}\right)^2 \\ &- 0.03188 \left(\log_{10} X_{\text{CO}_2}\right) + 0.001164 \left(\log_{10} X_{\text{CO}_2}\right)^2 \end{aligned} \tag{102}$$

where $X_{\text{H}_2\text{O}}$ and X_{CO_2} is proportional to the amount of water vapor or CO_2 in the path (dimensionless). These values are calculated by:

$$X_{\mathrm{CO_2}} = L \cdot \frac{273}{T} \cdot \frac{c_{\mathrm{CO_2}}}{335} \tag{103}$$

$$X_{\mathrm{H_2O}} = R_H \cdot L \cdot S_{\mathrm{mm}} \cdot \frac{2.88651 \times 10^{-2}}{T} \tag{104}$$

In these relationships, L is the path length (m) through which the radiative light must travel, T is the ambient temperature (K), $c_{\mathrm{CO_2}}$ is the concentration of CO_2 in the atmosphere (ppm, assumed to be 400 ppm), R_H is the fractional relative humidity (ranges from 0–1), and S_{mm} is the saturated water vapor pressure (mm Hg), estimated by the relationship:

$$S_{\mathrm{mm}} = \exp\left(10.386 - \frac{5132}{T}\right) \tag{105}$$

3.4.2. Jet Flame with Buoyancy Correction

A similar model to the jet/plume model described in Section 3.3.1 is also used to describe a flame. The model is described by Ekoto et al. [31]. The major difference between the jet/plume model and the flame model is that rather than the mole fraction, the mixture fraction, shown in Equation 33, is a conserved scalar. Similar assumptions are made for Gaussian profiles of the velocity and mixture fraction:

$$v = v_{cl} \exp\left(-\frac{r^2}{B^2}\right) \tag{106}$$

$$f = f_{cl} \exp\left(-\frac{r^2}{\lambda^2 B^2}\right) \tag{107}$$

with the conservation equations written as

x-centerline:

$$\frac{dx}{dS} = \cos\theta \tag{108}$$

y-centerline:

$$\frac{dy}{dS} = \sin\theta \tag{109}$$

continuity:

$$\frac{d}{dS}2\pi\int_0^\infty \rho v r dr = \rho_{amb} E \tag{110}$$

x-momentum:

$$\frac{d}{dS}2\pi\int_0^\infty \rho v^2 \cos\theta r dr = 0 \tag{111}$$

y-momentum:

$$\frac{d}{dS}\int_0^\infty \rho v^2 \sin\theta r dr = \int_0^\infty (\rho_{amb} - \rho) g r dr \tag{112}$$

mixture fraction:

$$\frac{d}{dS}2\pi\int_0^\infty \rho V f r dr = 0 \tag{113}$$

Note that energy conservation is not included in this formulation, but rather the mixture is assumed to be thermally perfect, with combustion calculations shown in Section 3.1.2. These calculations assume that the mixture is always in equilibrium (neglecting heat-losses), which results in a calculation of flame temperature and density as functions of mixture fraction similar to Figure 3-2 (with slight variations depending on the reactant temperature).

The Gaussian profiles in Equations 106 and 107 are numerically evaluated out to $5B$ (an estimate of ∞), along with the radial profiles of the density (based off of the mixture fraction), which can be plugged into Equations 108–113 and numerically integrated. This results in a system of 6 first order differential equations where the independent variable is S and the dependent variables are v_{cl}, B, θ, f_{cl}, x, and y. This system of equations is integrated from the starting point to the distance desired using an explicit Runge-Kutta method of order (4)5. Typically, the integration distance is the visible flame length, calculated using the correlations in Equations 95 and 96.

Similar to the nonreacting jet, entrainment in the jet flame is modeled as the sum of momentum and buoyancy contributions (Equation 77). However, rather than defining the buoyancy caused entrainment as before (Equation 79), buoyancy driven entrainment is calculated as

$$E_{buoy} = 2\pi\alpha_{buoy} g \sin\theta \frac{\int_0^\infty (\rho_{amb} - \rho) dr}{B v_{cl} \rho_{exit}} \tag{114}$$

The empirical constant for momentum driven entrianment in Equation 78 of 0.282, and empirical constant for buoyancy driven entrainment in Equation 114 (α_{buoy}) are also different for flames rather than unignited plumes/jets, with a value of 0.0342 for momentum driven entrainment, and $\alpha_{buoy} = 5.75 \times 10^{-4}$ [31].

3.4.3. Radiation From a Curved Flame

The radiative heat flux from the buoyancy corrected, curved flame is calculated by a weighted multi-source model, similar to that described by Hankinson and Lowesmith [53]. The heat flux at a point along the flame is calculated as

$$q = \tau S_{\text{rad}} \frac{V_F}{A_f} \tag{115}$$

where S_{rad} is calculated according to Equations 98–100, V_F is the view-factor, proportional to the heat flux transmitted to the observer, τ is the transmissivity, calculated by Equation 102, and A_f is the surface area of the flame. Contributions to the total heat flux are broken up into many (N, generally 50) points along the length of the curved flame, and the weighted average proceeds as

$$\tau \frac{V_F}{A_f} = \sum_{i=1}^{N} \frac{w_i \cos\beta_i}{4\pi D_i^2} \tau_i \tag{116}$$

where the emitter strength weighting parameter

$$w_i = \begin{cases} i w_1 & i \leq 0.75N \\ \left[n - \frac{n-1}{N-n-1}(i-(n+1)) \right] w_1 & i > 0.75N \end{cases} \tag{117}$$

with the constraint that $1 \leq n \leq N$ and $\sum_{i=1}^{N} w_i = 1$. In these equations, D and β are the distance and angle, respectively between the observer and unit normal to the point emitter.

3.4.4. Overpressure in Enclosures

If a confined mixture ignites, significant overpressures can develop within the enclosure or confinement area. Overpressure is calculated assuming that the cause of overpressure is the volume change on combustion pressurizing the enclosure. Within HyRAM+, the models described in Section 3.3.3 are used to calculate the volume of fuel within the layer and entire enclosure. It is assumed that all of the fuel within the flammability limits (in both the jet/plume and the accumulated layer) reacts, and the overpressure is calculated, following Bauwens and Dorofeev [54] as

$$\Delta p = p_0 \left(\left[\left(\frac{V_T + V_{\text{C}_\text{n}\text{H}_{2\text{n}+2}}}{V_T} \right) \left(\frac{V_T + V_{\text{stoich}}(\sigma - 1)}{V_T} \right) \right]^{\gamma} - 1 \right) \tag{118}$$

where p_0 is the initial pressure, V_T is the total volume of the enclosure, $V_{\text{C}_\text{n}\text{H}_{2\text{n}+2}}$ is the expanded volume of pure fuel following the release, V_{stoich} is the volume of a stoichiometric mixture of the consumed fuel, σ is the expansion ratio of a stoichiometric fuel-air mixture, and γ is the specific heat ratio of air. The expanded volume is given by $V_{\text{C}_\text{n}\text{H}_{2\text{n}+2}} = m_{\text{C}_\text{n}\text{H}_{2\text{n}+2}} / \rho_{\text{C}_\text{n}\text{H}_{2\text{n}+2}}$ where $m_{\text{C}_\text{n}\text{H}_{2\text{n}+2}}$

is the mass of fuel consumed and $\rho_{C_nH_{2n+2}}$ is the density of the fuel at ambient conditions. V_{stoich} is $V_{C_nH_{2n+2}}$ divided by the stoichiometric mole fraction of fuel.

3.4.5. Unconfined Overpressure

If an unconfined mixture ignites after a release has been flowing for some time, overpressures can be observed as the initial mixture burns. HyRAM+ has three different methods for calculating the overpressure. Each of these methods requires the calculations from an unconfined, unignited jet/plume, as described in Section 3.3.1. Each method calculates an overpressure and possibly impulse as a function of distance, R. We assume that the origin for the overpressure/impulse (distance from which R is measured) is near the center of the plume, estimated as $1/2$ the distance to the lower flammability limit along the jet streamline.

BST (Baker-Strehlow-Tang) The Baker-Strehlow-Tang (BST) model is based on blast curves that relate overpressure and impulse to the Mach flame speed [55]. The flammable mass of fuel within the unignited jet/plume is first found by volumetrically integrating the product of the mass fraction and density of the jet/plume that is within the flammability limits, or

$$m_{flam} = \int_{S=0}^{S=\infty} \left(\int_{r_{Y=Y_{UFL}}}^{r_{Y=Y_{LFL}}} \rho Y 2\pi r dr \right) dS. \tag{119}$$

The energy within the unignited mixture is related to the flammable mass through the relationship

$$E_{flam} = k_{reflection} m_{flam} \Delta H_c \tag{120}$$

where $k_{reflection}$ is a ground reflection factor (assumed to be 2). The scaled distance is related to the energy through the relationship

$$R^*_{BST} = \frac{R}{(E_{flam}/P_{\text{ambient}})^{(1/3)}}. \tag{121}$$

The scaled overpressure and impulse are related to the scaled distance, based on the Mach flame speed, as shown in Fig. 3-4.

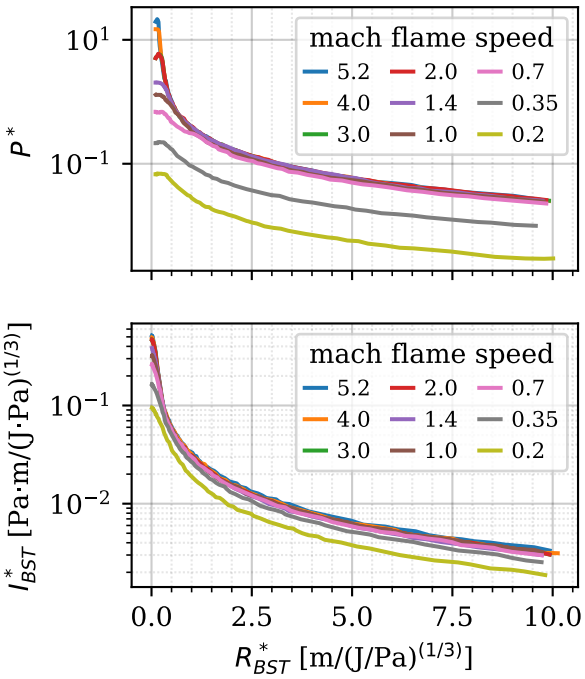

Figure 3-4 Mapping of scaled distance to scaled overpressure (top) and scaled impulse (bottom) for the BST unconfined overpressure model.

The scaled overpressure is the overpressure relative to ambient pressure ($P^* = P/P_{\text{ambient}}$), and the impulse is scaled by the flammable energy, ambient pressure, and speed of sound for air ($a_{\text{air}} = 340$ m/s) as

$$I^*_{BST} = \frac{I a_{\text{air}}}{(E_{flam} P^2_{\text{ambient}})^{(1/3)}}. \tag{122}$$

TNT equivalence The TNT equivalence method is based on the finding the mass of TNT that contains the same energy as the fuel being combusted [55]. The flammable mass of fuel within the jet/plume is found by volumetrically integrating the product of the mass fraction and density of the jet/plume that is within the flammability limits (see Eq. 119). A fraction of the flammable mass (the equivalence factor, set to 3% by default [55]) is presumed to combust, and the equivalent mass of TNT is calculated as

$$m_{TNT_{equiv}} = F_{equiv} \frac{m_{flam} \Delta H_c}{\Delta H_{c,TNT}}, \tag{123}$$

where F_{equiv} is the equivalence factor, and $\Delta H_{c,TNT} = 4.68$ MJ/kg, is the specific combustion energy in TNT. The scaled distance is related to the equivalent mass of TNT through the relationship

$$R^*_{TNT} = \frac{R}{m^{(1/3)}_{TNT_{equiv}}}, \tag{124}$$

and the scaled overpressure and impulse resulting from combustion are related to the scaled distance as shown by Fig. 3-5.

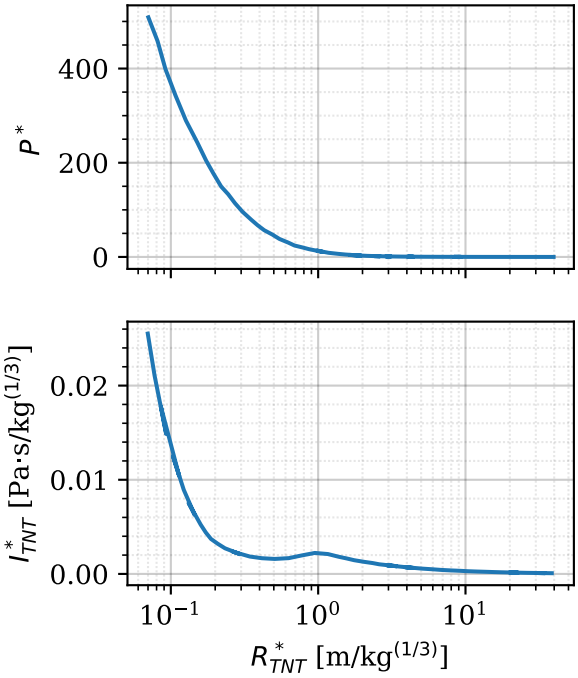

Figure 3-5 Mapping of scaled distance to scaled overpressure (top) and scaled impulse (bottom) for the TNT equivalence unconfined overpressure model.

The scaled overpressure is the overpressure relative to ambient pressure ($P^* = P/P_{\text{ambient}}$), and the impulse is scaled by the third root of the TNT mass, or

$$I^*_{TNT} = \frac{I}{m^{(1/3)}_{TNT_{equiv}}}. \tag{125}$$

Bauwens The Bauwens method for unconfined overpressure calcuation is based on the work of Bauwens and Dorfeev [56, 57]. The detonable mass within the unconfined jet/plume is calculated, and the overpressure is based on detonation of that mass of fuel. The detonation cell size, λ, is calculated for the entire jet/plume, based on fits to data from the detonation database [58]. The fits and data for different fuels are shown in Fig. 3-6.

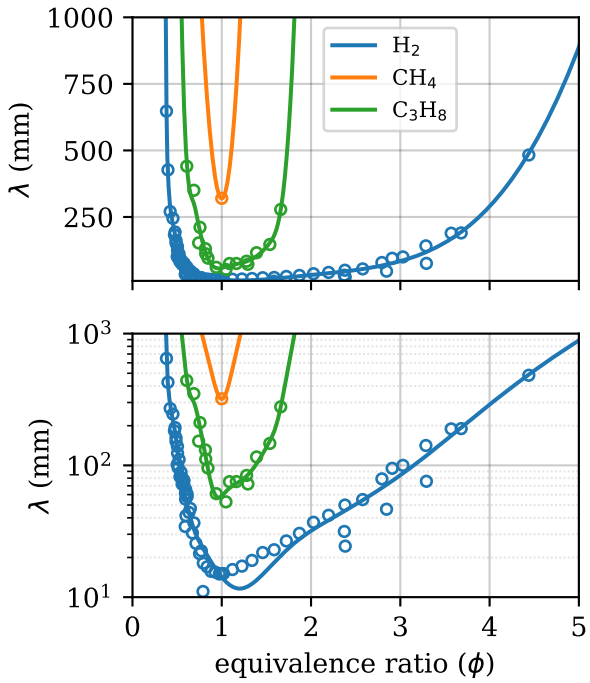

Figure 3-6 Detonation cell size data (points) from the detonation database [58] and fits to the data (lines) on a linear (top) and logarithmic (bottom) scale.

The gradient in the radial direction of the detonation cell size ($d\lambda/dr$) is found numerically, along with the number of cells that fit within the layer as

$$n_\lambda = \int_0^r \frac{dr}{\lambda(r)}. \tag{126}$$

Detonations are presumed to propagate in areas that are within the flammability limits, with a detonation cell size gradient less than 0.1 ($d\lambda/dr < 0.1$), and where there are at least 5 cells within the layer ($n_\lambda \geq 5$). The mass of fuel within the jet/plume that meets these constraints is calculated as the detonable mass (m_{det}). The dimensionless distance from the center of the detonable region is calculated as

$$R^* = R\left(\frac{P_{\text{ambient}}}{E}\right)^{(1/3)}, \tag{127}$$

where $E = m_{\text{det}}\Delta H_c$ is the energy of detonable fuel. Finally, the overpressure due to the detonable fuel is calculated as

$$P^* = \frac{P}{P_{\text{ambient}}} = \frac{0.34}{(R^*)^{(4/3)}} + \frac{0.062}{(R^*)^2} + \frac{0.0033}{(R^*)^3}. \tag{128}$$

There is currently no calculation of impulse for this model.

4. SUMMARY OF NUMERICAL METHODS

4.1. Python Calculation Methods

The Python modules in HyRAM+ utilize the NumPy and SciPy packages [59–61]. NumPy provides support for multi-dimensional arrays, mathematical functions of arrays, and some numerical linear algebra routines. SciPy provides a variety of numerical method routines including support for statistical distributions, numerical linear algebra, integration, interpolation, optimization, root-finding, ordinary differential equation solvers, and others. Plots in HyRAM+ are made using Matplotlib [62].

4.2. Leak Frequency Computations

Almost all of the computations for HyRAM+ are done in the Python code modules. However, the HyRAM+ QRA mode uses statistical distributions from Math.NET [63] for calculating the component release frequency mean and variance (see Section 2.4). This allows the leak frequency values to update quickly in the front-end without calling Python.

4.3. Unit Conversion

HyRAM+ enforces an immutable link between values and the units that define them. Input values are stored in the International System of Units (SI). Conversions are performed implicitly by the system. Therefore, the application is able to present data in units preferred by the user or more relevant in problem context, while being able to pass data to the Python calculation algorithms in the expected SI units. Table 4-1 contains the convertible units currently available in HyRAM+. Note that all pressure units are assumed to be absolute pressure, not gauge pressure.

Table 4-1 HyRAM+ Convertible Units

Unit Type	Units Available
Distance	m, cm, mm, in, ft, yd, mi, au
Area	m^2, cm^2, mm^2, ft^2, in^2, yd^2
Volume	cm^3, dm^3, dam^3, m^3, km^3, mm^3, μm^3, ft^3, in^3, yd^3, mi^3, L, μL, mL, dL, daL, kL, ML
Angle	radians, degrees
Energy	J, kWh, BTU
Time	s, ms, min, hr
Pressure	Pa, kPa, MPa, psi, atm, bar, J/m^3
Temperature	Celsius, Fahrenheit, Kelvin
Speed	m/s
Volumetric Flow Rate	m^3/s

This page intentionally left blank.

5. ENGINEERING TOOLKIT

This section describes the Engineering Toolkit, which uses the models described elsewhere in this report to perform simple calculations for properties of the different fuels.

5.1. Temperature, Pressure, and Density

The user can calculate one of the quantities temperature (T), pressure (P), or density (ρ) by specifying the other two. The algorithm uses the the CoolProp library [27] to perform the thermodynamic calculations (see Section 3.1.1).

5.2. Tank Mass

The user can calculate the mass (m) of fuel in a container by specifying the temperature (T), pressure (P), and volume (V) of the container.

$$m = \rho V \tag{129}$$

Where the density (ρ) is calculated using the CoolProp library [27] as described in Section 5.1.

5.3. Mass Flow Rate

The mass flow rate ($\dot{m}$) of a leak from a tank can be calculated for either a steady release or for a pressure blowdown of a tank. A "blowdown" describes the release of gas from a tank until the pressure reaches ambient, causing the mass flow to stop. This can be estimated from the temperature (T), pressure (P), and leak size ("Orifice Diameter", d) for a steady release, and also volume (V) for a blowdown case.

For a steady-state release, the mass flow rate ($\dot{m}$) is calculated using the density of the fluid (ρ), the velocity of the fluid through the orifice (v), and the area of the orifice (A)[8]:

$$\dot{m} = \rho v A \tag{130}$$

The area of the orifice is given by the diameter of the orifice (d):

$$A = \frac{\pi}{4} d^2 \tag{131}$$

The density and velocity of the fluid depend on the temperature (T) and pressure (P) of the tank and are calculated for the flowing fluid as described in Section 3.2.1. The output for the steady state case is the mass flow rate in kg/s.

[8] In many fluid flow calculations, a discharge coefficient is used to scale the mass flow through an orifice. As can be deduced from Eq. 130, the discharge coefficient for the Engineering Toolkit is assumed to be equal to 1.0.

For the blowdown case, the initial mass in the tank (m_0) is calculated (same as Section 5.2) by:

$$m_0 = \rho_0 V \tag{132}$$

where ρ_0 is the initial density of hydrogen in the tank (which depends on the initial temperature (T) and pressure (P) of the tank and is calculated as described in Section 5.1) and V is the volume of the tank.

The mass and energy flow equations (as described in Section 3.3.2) are then integrated until the the tank pressure is equal to ambient pressure (101,325 Pa). The output for the blowdown case is a combination plot of the mass in the tank, tank pressure, mass flow rate, and temperature over time, as well as the total time needed for the tank to empty.

5.4. TNT Mass Equivalence

The TNT mass equivalence ($m_{\text{TNT equivalent}}$) can be calculated using the flammable vapor release mass (m_{fuel}), the explosive energy yield (Y, 0–100%), and the net heat of combustion (ΔH_c). This is calculated as:

$$m_{\text{TNT equivalent}} = \frac{m_{\text{fuel}} \times Y \times \Delta H_c}{4500 \text{ kJ/kg}_{\text{TNT}}} \tag{133}$$

The heat of combustion for hydrogen, methane, and propane are $\Delta H_{c,\text{ hydrogen}} = 120$ MJ/kg [33, 34], $\Delta H_{c,\text{ methane}} = 50.0$ MJ/kg, $\Delta H_{c,\text{ propane}} = 46.4$ MJ/kg. The TNT mass equivalence equation is taken from NUREG-1805 [64].

REFERENCES

[1] B. D. Ehrhart, E. S. Hecht, K. M. Groth, J. T. Reynolds, M. L. Blaylock, and E. E. Carrier, "Hydrogen Risk Assessment Models (HyRAM) Version 3.1 Technical Reference Manual," Sandia National Laboratories, Tech. Rep. SAND2021-5812, May 2021.

[2] Center for Chemical Process Safety (CCPS), *Guidelines for Chemical Process Quantitative Risk Analysis*. American Institute of Chemical Engineers, 1999.

[3] T. Aven, *Foundations of risk analysis*. John Wiley & Sons, 2003.

[4] M. Modarres, *Risk Analysis in Engineering: Techniques, Tools, and Trends*. CRC Press, 2006.

[5] SFPE, "SFPE engineering guide to performance-based fire protection analysis and design of buildings," National Fire Protection Association, Quincy, MA, USA, Tech. Rep., 2007.

[6] S. E. Rose, S. Flamberg, and F. Leverenz, *Guidance Document for Incorporating Risk Concepts into NFPA Codes and Standards*. Fire Protection Research Foundation, March 2007.

[7] J.-E. Vinnem, *Offshore Risk Assessment: Principles, Modelling and Applications of QRA Studies*, 2nd ed. Springer, 2007.

[8] T. Aven, *Quantitative risk assessment: the scientific platform*. Cambridge University Press, 2011.

[9] B. D. Ehrhart, D. Brooks, A. B. Muna, and C. LaFleur, "Evaluation of risk acceptance criteria for transporting hazardous materials," DOT Federal Railway Administration, Tech. Rep. DOT/FRA/ORD-20/06, February 2020.

[10] B. D. Ehrhart, E. S. Hecht, and J. A. Mohmand, "Validation and comparison of HyRAM physics models," Sandia National Laboratories, Tech. Rep. SAND2021-5811, May 2021.

[11] S. Egbert, X. Li, M. L. Blaylock, and E. Hecht, "Mixing of liquid methane releases." Sandia National Lab.(SNL-CA), Livermore, CA (United States), Tech. Rep. SAND2018-13757R, 2018.

[12] M. L. Blaylock, E. Hecht, and C. Jordan, "Validation of the altram physics models for use with compressed natural gas." Sandia National Laboratories, Tech. Rep. SAND2019-13408, June 2020. [Online]. Available: https://www.osti.gov/biblio/1763555

[13] J. G. Shum, , E. S. Hecht, and M. L. Blaylock, "Validation of the hyram+ physics models for use with propane," Sandia National Lab.(SNL-CA), Livermore, CA (United States), Tech. Rep. SAND2021-3244, 2021.

[14] K. M. Groth, J. L. LaChance, and A. P. Harris, "Early-stage quantitative risk assessment to support development of codes and standard requirements for indoor fueling of hydrogen vehicles," Sandia National Laboratories, Tech. Rep. SAND2012-10150, November 2012.

[15] A. V. Tchouvelev, "Knowledge gaps in hydrogen safety: A white paper," International Energy Agency Hydrogen Implementing Agreement Task 19, Tech. Rep., January 2008.

[16] J. LaChance, W. Houf, B. Middleton, and L. Fluer, "Analyses to support development of risk-informed separation distances for hydrogen codes and standards," Sandia National Laboratories, Tech. Rep. SAND2009-0874, March 2009.

[17] A. Glover, A. Baird, and D. Brooks, "Final report on hydrogen planthazards and risk analysissupporting hydrogen plant sitingnear nuclear power plants," Sandia National Laboratories, Tech. Rep. SAND2020-7946, July 2020.

[18] D. M. Brooks, B. D. Ehrhart, and C. LaFleur, "Development of liquid hydrogen leak frequencies using a bayesian update process," in *2021 International Conference on Hydrogen Safety*, September 2021.

[19] G. W. Mulcahy, D. M. Brooks, and B. D. Ehrhart, "Using bayesian methodology to estimate liquefied natural gas leak frequencies," Sandia National Laboratories, Tech. Rep. SAND2021-4905, April 2021.

[20] J. LaChance, A. Tchouvelev, and A. Engebø, "Development of uniform harm criteria for use in quantitative risk analysis of the hydrogen infrastructure," *International Journal of Hydrogen Energy*, vol. 36, no. 3, pp. 2381–2388, February 2011.

[21] N. A. Eisenberg, C. J. Lynch, and R. J. Breeding, "Vulnerability model. A simulation system for assessing damage resulting from marine spills," U.S. Coast Guard, Tech. Rep. SA/A-015 245, 1975.

[22] C. K. Tsao and W. W. Perry, "Modifications to the vulnerability model: a simulation system for assessing damage resulting from marine spills," U.S. Coast Guard, Tech. Rep. ADA 075 231, 1979.

[23] TNO, "Methods for the determination of possible damage," The Netherlands Organization of Applied Scientific Research (TNO), Tech. Rep. CPR 16E, 1992.

[24] F. P. Lees, "The assessment of major hazards: a model for fatal injury from burns," *Process Safety and Environmental Protection*, vol. 72, no. 3, pp. 127–134, 1994.

[25] HSE, *Major hazard aspects of the transport of dangerous substances*. UK Health and Safety Executive, 1991.

[26] UK Health and Safety Executive, "Methods of approximation and determination of human vulnerability for offshore major accident hazard assessment," UK Health and Safety Executive, Tech. Rep., 2010.

[27] I. H. Bell, J. Wronski, S. Quoilin, and V. Lemort, "Pure and Pseudo-pure Fluid Thermophysical Property Evaluation and the Open-Source Thermophysical Property Library CoolProp," *Industrial & Engineering Chemistry Research*, vol. 53, no. 6, pp. 2498–2508, February 2014.

[28] J. W. Leachman, R. T. Jacobsen, S. G. Penoncello, and E. W. Lemmon, "Fundamental equations of state for parahydrogen, normal hydrogen, and orthohydrogen," *Journal of Physical and Chemical Reference Data*, vol. 38, no. 3, pp. 721–748, September 2009.

[29] U. Setzmann and W. Wagner, "A new equation of state and tables of thermodynamic properties for methane covering the range from the melting line to 625 K at pressures up to 100 MPa," *Journal of Physical and Chemical Reference Data*, vol. 20, no. 6, pp. 1061–1155, 1991.

[30] E. W. Lemmon, M. O. McLinden, and W. Wagner, "Thermodynamic properties of propane. III. A reference equation of state for temperatures from the melting line to 650 K and pressures up to 1000 MPa," *Journal of Chemical & Engineering Data*, vol. 54, no. 12, pp. 3141–3180, 2009.

[31] I. W. Ekoto, A. J. Ruggles, L. W. Creitz, and J. X. Li, "Updated jet flame radiation modeling with buoyancy corrections," *International Journal of Hydrogen Energy*, vol. 39, no. 35, pp. 20 570–20 577, December 2014.

[32] National Institute of Standards and Technology. NIST Chemistry WebBook, SRD 69. [Online]. Available: https://webbook.nist.gov/chemistry/

[33] F. P. Lees, *Lees' Loss Prevention in the Process Industries*, 3rd ed., S. Mannan, Ed. Elsevier Science & Technology, 2005.

[34] M. J. Hurley, D. T. Gottuk, J. R. H. Jr., K. Harada, E. D. Kuligowski, M. Puchovsky, J. L. Torero, J. M. W. Jr., and C. J. Wieczorek, Eds., *SFPE Handbook of Fire Protection Engineering*, 5th ed. Springer, New York, NY, 2016.

[35] M.-S. Chung, S.-B. Park, and H.-K. Lee, "Sound speed criterion for two-phase critical flow," *Journal of Sound and Vibration*, vol. 276, no. 1, pp. 13–26, 2004.

[36] K. B. Yüceil and M. V. Ötügen, "Scaling parameters for underexpanded supersonic jets," *Physics of Fluids*, vol. 14, no. 12, pp. 4206–4215, October 2002.

[37] A. D. Birch, D. J. Hughes, and F. Swaffield, "Velocity decay of high pressure jets," *Combustion Science and Technology*, vol. 52, no. 1-3, pp. 161–171, 1987.

[38] A. D. Birch, D. R. Brown, M. G. Dodson, and F. Swaffield, "The structure and concentration decay of high pressure jets of natural gas," *Combustion Science and Technology*, vol. 36, no. 5-6, pp. 249–261, 1984.

[39] B. C. R. Ewan and K. Moodie, "Structure and velocity measurements in underexpanded jets," *Combustion Science and Technology*, vol. 45, no. 5-6, pp. 275–288, 1986.

[40] V. Molkov, D. Makarov, and M. Bragin, "Physics and modelling of under-expanded jets and hydrogen dispersion in atmosphere," in *Proceedings of the 24th international conference on interaction of intense energy fluxes with matter*, March 1-6 2009.

[41] W. Houf and W. Winters, "Simulation of high-pressure liquid hydrogen releases," *International Journal of Hydrogen Energy*, vol. 38, no. 19, pp. 8092–8099, June 2013.

[42] W. S. Winters, "Modeling leaks from liquid hydrogen storage systems," Sandia National Laboratories, Tech. Rep. SAND2009-0035, January 2009.

[43] G. Abraham, "Horizontal jets in stagnant fluid of other density," *Journal of the Hydraulics Division*, vol. 91, no. 4, pp. 139–154, 1965.

[44] W. Houf and R. Schefer, "Analytical and experimental investigation of small-scale unintended releases of hydrogen," *International Journal of Hydrogen Energy*, vol. 33, no. 4, pp. 1435–1444, February 2008.

[45] M. Hosseini, I. Dincer, G. Naterer, and M. Rosen, "Thermodynamic analysis of filling compressed gaseous hydrogen storage tanks," *International Journal of Hydrogen Energy*, vol. 37, no. 6, pp. 5063–5071, March 2012.

[46] B. Lowesmith, G. Hankinson, C. Spataru, and M. Stobbart, "Gas build-up in a domestic property following releases of methane/hydrogen mixtures," *International Journal of Hydrogen Energy*, vol. 34, no. 14, pp. 5932–5939, July 2009.

[47] W. Houf and R. Schefer, "Predicting radiative heat fluxes and flammability envelopes from unintended releases of hydrogen," *International Journal of Hydrogen Energy*, vol. 32, no. 1, pp. 136–151, January 2007.

[48] S. R. Turns and F. H. Myhr, "Oxides of nitrogen emissions from turbulent jet flames: Part i—fuel effects and flame radiation," *Combustion and Flame*, vol. 87, no. 3, pp. 319–335, 1991.

[49] R. Schefer, W. Houf, B. Bourne, and J. Colton, "Spatial and radiative properties of an open-flame hydrogen plume," *International journal of hydrogen energy*, vol. 31, no. 10, pp. 1332–1340, 2006.

[50] P. P. Panda and E. S. Hecht, "Ignition and flame characteristics of cryogenic hydrogen releases," *International Journal of Hydrogen Energy*, vol. 42, no. 1, pp. 775–785, January 2017.

[51] A. Molina, R. W. Schefer, and W. G. Houf, "Radiative fraction and optical thickness in large-scale hydrogen-jet fires," *Proceedings of the Combustion Institute*, vol. 31, no. 2, pp. 2565–2572, January 2007.

[52] F. D. Wayne, "An economical formula for calculating atmospheric infrared transmissivities," *Journal of Loss Prevention in the Process Industries*, vol. 4, no. 2, pp. 86 – 92, January 1991.

[53] G. Hankinson and B. J. Lowesmith, "A consideration of methods of determining the radiative characteristics of jet fires," *Combustion and Flame*, vol. 159, no. 3, pp. 1165–1177, March 2012.

[54] C. Bauwens and S. Dorofeev, "CFD modeling and consequence analysis of an accidental hydrogen release in a large scale facility," *International Journal of Hydrogen Energy*, vol. 39, no. 35, pp. 20 447–20 454, December 2014.

[55] Center for Chemical Process Safety, *Guidelines for Vapor Cloud Explosion, Pressure Vessel Burst, BLEVE, and Flash Fire Hazards*. John Wiley & Sons Ltd., 2010.

[56] C. Bauwens and S. B. Dorofeev, "Modeling detonation limits for arbitrary non-uniform concentration distributions in fuel–air mixtures," *Combustion and Flame*, vol. 221, pp. 338–345, 2020.

[57] C. R. L. Bauwens and S. B. Dorofeev, "Quantifying the potential consequences of a detonation in a hydrogen jet release," in *Proceedings of the International Conference on Hydrogen Safety (ICHS 2019)*, Adelaide (Austrailia), September 24 - 26 2019, pp. 612–623.

[58] Califiornia Insitute of Technology and J. E. Shepherd. Detonation Database. [Online]. Available: https://shepherd.caltech.edu/detn_db/html/db_10.html

[59] T. E. Oliphant, *A guide to NumPy*. Trelgol Publishing USA, 2006, vol. 1.

[60] S. Van Der Walt, S. C. Colbert, and G. Varoquaux, "The numpy array: a structure for efficient numerical computation," *Computing in Science & Engineering*, vol. 13, no. 2, p. 22, 2011.

[61] P. Virtanen, R. Gommers, T. E. Oliphant, M. Haberland, T. Reddy, D. Cournapeau, E. Burovski, P. Peterson, W. Weckesser, J. Bright, S. J. van der Walt, M. Brett, J. Wilson, K. Jarrod Millman, N. Mayorov, A. R. J. Nelson, E. Jones, R. Kern, E. Larson, C. Carey, İ. Polat, Y. Feng, E. W. Moore, J. VanderPlas, D. Laxalde, J. Perktold, R. Cimrman, I. Henriksen, E. A. Quintero, C. R. Harris, A. M. Archibald, A. H. Ribeiro, F. Pedregosa, P. van Mulbregt, and SciPy 1.0 Contributors, "SciPy 1.0: Fundamental Algorithms for Scientific Computing in Python," *Nature Methods*, vol. 17, pp. 261–272, 2020.

[62] J. D. Hunter, "Matplotlib: A 2D graphics environment," *Computing in Science & Engineering*, vol. 9, no. 3, pp. 90–95, 2007.

[63] Math.net numerics. [Online]. Available: http://numerics.matdotnet.com

[64] N. Iqbal and M. H. Salley, "Fire Dynamics Tools (FDTs): Quantitative Fire Hazard Analysis Methods for the U.S. Nuclear Regulatory Commission Fire Protection Inspection Program," U.S. Nuclear Regulatory Commission, Washington, DC, Tech. Rep. NUREG-1805, December 2004.

DISTRIBUTION

Email—Internal

Name	Org.	Sandia Email Address
Ethan Hecht	8367	ehecht@sandia.gov
Brian Ehrhart	8854	bdehrha@sandia.gov
Ben Schroeder	8854	bbschro@sandia.gov
Myra Blaylock	8751	mlblayl@sandia.gov
Chris LaFleur	8854	aclafle@sandia.gov
Scott Sanborn	8854	sesanbo@sandia.gov
Mike Starr	8853	mjstarr@sandia.gov
Kristin Hertz	8367	klhertz@sandia.gov
CA Technical Library	8551	cateclib@sandia.gov

Email—External

Name	Company Email Address	Company Name
Katrina Groth	kgroth@umd.edu	University of Maryland
Laura Hill	laura.hill@ee.doe.gov	DOE EERE HFTO
Mark Smith	mark.smith@ee.doe.gov	DOE EERE VTO
Michael Laughlin	michael.laughlin@ee.doe.gov	DOE EERE VTO
Thach Nguyen	thach.d.nguyen@dot.gov	DOT PHMSA

Sandia National Laboratories

Sandia National Laboratories is a multimission laboratory managed and operated by National Technology & Engineering Solutions of Sandia LLC, a wholly owned subsidiary of Honeywell International Inc., for the U.S. Department of Energy's National Nuclear Security Administration under contract DE-NA0003525.